

TALLINN UNIVERSITY OF TECHNOLOGY  
THESIS OF MATERIALS ENGINEERING

**Fatigue Performance and Mechanical Reliability of  
Cemented Carbides**

IRINA PREIS

TALLINN 2004

Faculty of Mechanical Engineering  
Department of Materials Engineering  
TALLINN UNIVERSITY OF TECHNOLOGY

Dissertation is accepted for the defence of the degree of Doctor of Philosophy in Engineering on November 25, 2004

Supervisor:

Prof. Dr. Jakob Kübarsepp, Faculty of Mechanical Engineering

Adviser: Dr. Heinrich Klaasen, Faculty of Mechanical Engineering

Opponents:

Dr. Michal Besterčí, Institute of Materials Research of SAS, Kosice, Slovak Republic

Dr. Mart Viljus, Tallinn University of Technology, Estonia

Commencement: December 28, 2004

Declaration

I declare that the current thesis is my original unaided work. It is being submitted for the Degree of Doctor of Philosophy in Engineering at Tallinn University of Technology. It has not been submitted before for any degree or examination in any other university.

Signature:

Date:

© Irina Preis 2004

ISSN

ISBN

## **PREFACE**

The author gratefully acknowledges the Estonian Science Foundation, The Ministry of Education and Research of Estonia, Development Fund of Tallinn University of Technology and CIMO Foundation (Finland) for financial support of the present research.

The author would like to express her deepest gratitude to her supervisor, Prof. Dr. Jakob Kübarsepp, for fruitful discussions and sharing academic knowledge, for his permanent support during last six years of our productive collaboration. I also would like to thank Dr. Heinrich Klaasen for the encouragement of my doctoral studies, for his ideas in planning and evaluation of testing procedures. I would also like to thank my student and colleague MSc. Fjodor Sergejev for his help, contribution and activity in our research.

I would also like to give my special thanks to Prof. Dr. Gary Marquis, Head of Laboratory of Steel Structures of Lappeenranta University of Technology in Finland for his assistance and guidance helped in numerous technical issues.

I would like to thank my adviser in a field of accelerated testing approach Dr. Viktor Strizhak for his guidance and collaboration.

Special acknowledgements are given to the Testing Laboratory of the Department of Materials Engineering, Tallinn University of Technology and personally to the Head of Laboratory MSc. Riho Päärsoo and my colleague MSc. Renno Veithal for the guidance and support.

I would also like to thank my colleague MSc. Rainer Traksmäa, from The Materials Research Center of Tallinn University of Technology for his assistance and support in microfractographic investigations done.

I wish to express my most gratitude to my family and friends for their continuous direct and indirect support, patience, understanding and encouragement on the different stage of this work.

## **KOKKUVÕTE**

Uuriti erineva koostise ja struktuuriga kermetite (WC-kõvasulamid, TiC-kermised) töövõimet ja purunemismehhanismi tsüklilise (väsimus, stantsimine) koormamise tingimustes.

Arendati välja kiirendatud väsimuse tugevuse hindamise meetod kermetite töövõime hindamiseks ning näideti et materjali vastupanu väsimuslikule purunemisele määrab ühelt poolt tema väsimuspiir ja teiselt tema väsimustundlikkus (Wöhler-kõvera kalle).

Viidi läbi kermetite väsimus käitumise statistiline arutelu selgitamiseks välja nende Weibull modulite erinevused ning viimaste seos väsimustundlikusega.

Viidi läbi uuritavate kermetite eksploatatsioonilised katsed, selgitamiseks välja nende töövõime (kulumiskindlus) survega töötlemise operatsioonides (lehtstantsimisel) ja selle seos väsimusega.

Näideti, et suure töövõimega (stantsimis eaga) kermetit iseloomustab kõrge vastupanu adhesioonkulumisele ja väike väsimustundlikkus.

Viidi läbi mikrostruktuursed (SEM) ja röntgenstruktuursed (XRD) uuringud ning selgitati välja purunemismehhanismi erinevused ja sarnasused erinevatel kermetitel väsimusliku (tsüklilise) ja monotoonse koormamise tingimustes.

## **ABSTRACT**

The fatigue performance of cemented carbides with different composition, structure and properties has been investigated. It was shown that the differences in wear resistance between cermet materials with equal hardness and volume fraction of binder content can be attributed to differences in their resistance to fracture under cyclic loading conditions.

The accelerated fatigue testing procedure was designed and applied to assess the fatigue characteristics of selected materials. The important constitutive material constants for two major cemented carbides WC- and TiC- base utilised as tool materials in metal forming operations were calculated using an accelerated testing approach.

Standard fatigue testing in three-point bending showed that the resistance of materials tested to the damage processes under cyclic loading is much lower than that under monotonic one. The different slopes of the Wöhler plots expressed the different fatigue sensitivity of material structure. The estimated endurance limits and Weibull statistics were presented as well.

The durability tests carried out as the service condition tests showed that the blanking performance of the cemented carbides is controlled by their resistance to adhesive wear (primarily that of its binder) and to the propagation of fatigue cracks.

The statistical considerations of fatigue behavior were directed to explain the differences in Weibull modulus numbers for different testing schemes (tension, four point and three point bending loading), which are characterized by the differences in the stress field uniformity.

The microfractography studies by means of SEM and XRD analysis of fatigued and worn surfaces revealed the certain similarities in the micromechanisms of fatigue and wear. At the same time, an important aspect of accumulation of the elastic strain energy and plastic deformation (at cycling and monotonic loading) of different carbide phases explains the difference in their fatigue performance. The latter statement confirms that mechanical and service reliability of TiC-base cemented carbides can be compared with that of traditional tungsten carbide composites in spite of the lower magnitudes of mechanical characteristics, such as transverse rupture strength, proof stress and Young's modulus.

## TABLE OF CONTENT

<b>PREFACE</b> .....	<b>3</b>
<b>KOKKUVÕTE</b> .....	<b>4</b>
<b>ABSTRACT</b> .....	<b>5</b>
<b>TABLE OF CONTENT</b> .....	<b>6</b>
<b>LIST OF PUBLICATIONS</b> .....	<b>7</b>
<b>THE AUTHOR’S CONTRIBUTION TO PUBLICATIONS</b> .....	<b>8</b>
<b>INTRODUCTION</b> .....	<b>9</b>
<b>1 REVIEW OF FATIGUE DATA OF CEMENTED CARBIDES</b> .....	<b>11</b>
1.1 Fatigue testing approaches .....	11
1.2 Materials and testing procedures .....	12
1.3 Fatigue crack growth behaviour of cemented carbides .....	17
1.4 Microstructural aspects and fractography of fatigue crack growth in cemented carbides .....	20
1.5 Mechanical and tribological behaviour of cemented carbides .....	22
1.6 Statistical consideration of cemented carbides fatigue performance .....	24
1.7 Objectives and strategies .....	27
<b>2 EXPERIMENTAL PROGRAM</b> .....	<b>28</b>
2.1 Materials .....	28
2.2 Accelerated fatigue testing .....	30
2.3 Wear testing .....	32
2.4 Fatigue testing.....	33
2.5 Durability testing in blanking .....	35
2.6 Fatigue and bending strength: related fractography .....	35
<b>3 STATISTICAL ASPECTS OF FATIGUE PERFORMANCE AND ENDURANCE LIMIT PREDICTION</b> .....	<b>40</b>
3.1 Statistical strength, testing procedures and Weibull modulus.....	40
3.2 Prediction of the lower bound of the scatter in fatigue strength: Murakami approach .....	41
<b>CONCLUSIONS</b> .....	<b>43</b>
<b>REFERENCES</b> .....	<b>45</b>
<b>SYMBOLS AND ABBREVIATIONS</b> .....	<b>48</b>
<b>APPENDIX A</b> .....	<b>50</b>
<b>APPENDIX B</b> .....	<b>61</b>
<b>CURRICULUM VITAE (CV)</b> .....	<b>62</b>
<b>ELULOOKIRJELDUS (CV)</b> .....	<b>65</b>

## LIST OF PUBLICATIONS

The present dissertation is based on the following papers, which are referred to in the text by their Roman numerals I-V. As some of the results of recent research have not been published yet, this thesis was substantially enlarged.

- I. Preis, I., Kübarsepp, J. and Strizhak, V. - Preliminary assessment of durability of hardmetals and cermets. *Proceedings of the 3<sup>rd</sup> International Conference on Industrial Engineering – New Challenges to SME*, April 27-29, 2000, Tallinn, Estonia, pp.175-178.
- II. Preis, I. - Statistical strength of brittle materials: test methods and Weibull modulus. *Proceedings of 2<sup>nd</sup> International Conference - New Challenges to SME*, April 25-27, 2002, Tallinn, Estonia, pp.205-208.
- III. Klaasen, H., Kübarsepp, J. and Preis, I., - Wear behaviour, durability and cyclic strength of TiC-base cermets. - *Material Science and Technology*, 20, August, 2004, pp.1006-1010.
- IV. Klaasen, H., Kübarsepp, J. and Preis, I. - Toughness and durability of cemented carbides. *Proceedings of the International Conference on deformation and fracture of structural PM materials*, September 15-18, 2002, Slovak Republic, IMR SAS – European Powder Metallurgy Association, Kosice, Vol. 1, pp.77-83.
- V. Klaasen, H., Kübarsepp, J., and Preis, I. - Durability of advanced TiC-base cermets. *Proceedings of the Estonian Academy of Science*, 2003, 9, 4, pp.272-280.

In addition to this, the results of the research have been discussed on scientific workshops in Estonia and Finland.

In the Appendix B of this thesis, copies of the articles have been included. Reprints of papers were made with permission from the publisher.

## **THE AUTHOR'S CONTRIBUTION TO PUBLICATIONS**

The contribution of the author of present thesis into the papers listed above is as follows:

I The author fulfilled the experimental program, including experiments and analysis, systematically analyzed obtained results and participated in writing the paper.

II The author developed the theoretical approach and wrote the paper.

III The author herself obtained data of standard fatigue testing under supervision and cooperation with co-authors.

IV The author contributed by data obtained for fatigue performance and data concerning microfractography of failure.

V The author herself obtained data of standard fatigue testing under supervision and cooperation with co-authors.

## INTRODUCTION

The problem of the fatigue strength estimation of wear resistant cemented carbides, particularly hard metals containing natural defects, inclusions or inhomogeneities is of great importance from both a scientific or industrial point of view. These materials are related to so-called “structurally brittle” materials group. Therefore, designers are often hesitant to design components with brittle materials despite advantages regarding strength, weight and resistance to harsh mechanical loads, thermal and chemical environment. In this context, the research presented is the next attempt to enlarge the knowledge concerned time-dependent degradation of composites under alternating stresses.

Thanks to the group of scientists at Erlangen-Nürnberg University rebirth in interest in hard metal fatigue has been detected in the last few decades. The majority of the experimental work has been done using constant amplitude loading at short and long spectrum of materials life.

The obtained data show distinct differences of hard metal behavior under static and alternating loading. Nevertheless, very restricted aspects of the behavior of cemented carbides consisting of brittle ceramics embedded in a ductile binder phase were considered in some investigations in the past, which dealt with the fatigue resistance (Kreimer, 1971; Loshak, 1984; Shleikofer *et al.*, 1995 and 1996 etc.), fatigue crack growth (Torres *et al.*, 2000 and Llanes *et al.*, 2002), interrelations of fatigue crack growth and microstructure, influence of the microstructure and of the conditions of the surface on the fatigue performance, the influence of the plastic zone at the crack tip on the fatigue and crack resistance (Suresh, 1991).

More recent investigations of the fatigue of cemented carbides show that irreversible microscopic changes (micro-crack formation, phase transformation, phase boundary sliding and pore nucleation during fatigue processes) occur in front of the crack tip, analogous to the irreversible sliding processes during the fatigue of ductile materials. In addition different processes, caused by crack closure, crack bridging, and friction of opposite crack surfaces, have an influence on the fatigue crack growth. Especially, the latter processes are clearly different in the same materials under static or monotonously increasing loads.

The main goal of this work is to determine and compare the fatigue behaviour of the major groups of hardmetals: WC-based and TiC-based alloys. The research includes also an overview of the current experimental program, the most significant results in ‘endurance limit’ determination and in the fatigue sensitivity assessment. The aspects of statistical strength of materials are also the point of interest – the main Weibull distribution parameters are quantified for both static and cyclic fractures.

In order to evaluate quantitatively the effects of defects and inclusions on the fatigue strength of cemented carbides, Murakami (2002) method firstly was applied. The results of equating the lower band of scatter of endurance limit on the basis of binder Vicker’s hardness and geometric parameter  $\sqrt{area}_{max}$  showed its excellent

convergence with experimental data received from both testing procedures standard fatigue tests and accelerated fatigue ones.

Most experimental data on fatigue performance of hard metals and cermets are directed toward the sheet metals forming – blanking operations. Particularly, the TiC-FeNi composites, developed by the group of Laboratory of Powder Metallurgy in Tallinn University of Technology, are the promising candidates for the blanking dies. The observations on functional testing of these materials in the service conditions (blanking) are also presented. The relationship between the main mechanical characteristics like hardness, fracture toughness, plasticity, bending strength, wear resistance and fatigue ones is in-depth study. Microstructural investigations of the fatigue fracture are included in this work.

# 1 REVIEW OF FATIGUE DATA OF CEMENTED CARBIDES

## 1.1 Fatigue testing approaches

Fatigue data of cemented carbides (hard metals) are extremely limited. While certain stress vs. life (S/N) data has been developed for basic grades, only a few studies of the cyclic constitutive behavior of these alloys have been published.

As a rule, fatigue testing of structural materials is introduced within the bounds of three main approaches:

- stress-life approach,
- strain-life approach,
- fracture mechanics approach (fatigue crack growth).

For the most part, the stress-life approach is chosen like a major testing procedure for cemented carbides because of the obvious difficulties in measuring and monitoring strain during testing (Suresh, 1991). The problem in strain-life fatigue testing is the feature of a brittle material characterized by very little plastic flow that occurs in the specimen prior to failure. A fracture mechanics approach was used to develop a suitable phenomenological fatigue law (Sigl *et al.*, 1987). Main applications of cemented carbides include cases where they are subjected primarily to compressive stresses. Failure in compression is less catastrophic than in tension, and in some aspects qualitative resemblance with metal plasticity is observed. Therefore, the mechanics of cracks at present focuses on the numerical simulation of cracks coalescence under the loading conditions of Modes I and II. Crack propagation in the ductile binder of WC-based grades is simulated using different modelling strategies (Kenny *et al.*, 1971).

The development of the devices assigned for fatigue endurance data of the hard metals requires that certain specific application conditions be taken into account, in which the mechanical behaviour of hardmetals differs from other alloys. Main conditions may be listed as follows:

- hard metals exhibit much lower resistance towards tensile stresses than to compressive ones. Therefore, the influence of microstructural defects on material strength can be observed much more effectively in tension than in compression,
- the sensitivity of microstructure caused by material heterogeneity (two phases – hard particle-phase and ductile binder phase),
- very high magnitudes of Young's modulus (from 470 up to 670 GPa). It means that there are no any visible residual strains of bulk specimen during the testing procedure,
- the brittle manner of fracture and the presence of various defects (pores, inclusions etc.) on the microstructural level. It governs to statistical analysis for the real-valued assessment of fatigue characteristics. Consequently, the large amount of specimens must be tested (up to three times more than for steel fatigue investigations),

- some parts of hard metal tools are subjected to impact-bending loading in the service conditions (dies, punches, mining tools, cutting tools etc.). A number of hard metal tools are prone to damage by cyclic loading (Brookes, 1992).

These considerations were the basis of design and development of special rigs for the fatigue testing of cemented carbides.

## 1.2 Materials and testing procedures

Earlier investigations deal with fatigue testing of WC-Co alloys with different contents of Co phase under three-point bending (3PB) loading conditions (Kreimer, 1971) at ambient temperature. The coefficient of cyclic asymmetry  $R$  was 0.1. The maximum fracture stress was measured on the basis of  $5 \cdot 10^6$  cycles. The fatigue data obtained (Fig.1.1) show that the higher the Co-binder content (wt.%) the higher the endurance limit of the grade.

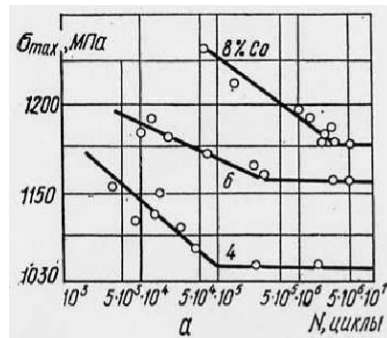


**Figure 1.1. Fatigue curves (Wöhler plots) for WC-Co with different cobalt content (Kreimer, 1971)**

The influence of carbide grain size was also established: the decrease of the endurance limit was related to the decrease of grain size of carbide phase or to the duration of WC and Co powder milling. The endurance limits data are presented in Table 1.1.

**Table 1.1 Hardness  $HRA$ , transverse rupture strength  $R_{TZ}$  and endurance limits  $S_e$  of H4, H6 and H8 grades (Kreimer, 1971)**

Grade	Hardness ( $HRA$ )	$R_{TZ}$ (MPa)	Endurance limit $S_{e, 5 \cdot 10^6}$ (MPa)
H4 (WC-4% Co)	90	1400	$\approx 1050$
H6 (WC-6% Co)	89	1470	$\approx 1160$
H8 (WC-8%Co)	88	1510	$\approx 1210$

It was assumed that the linear correlation between fatigue endurance limit and static strength in tension also exists. The distinctive features of Kreimer's work were the flat regions of the fatigue curves that are parallel to  $(\log N)$  axis. This fact shows the

possibility of existence of a fatigue limit (physical endurance limit) for hard metals. WC-Co alloys with 6, 12, 20 and 25 wt.% Co content were subjected to torsion-bending cyclic loading. But the majority of fatigue curves obtained from later investigations (Loshak, 1971) showed an evident absence of any flat regions (Fig.1.2).

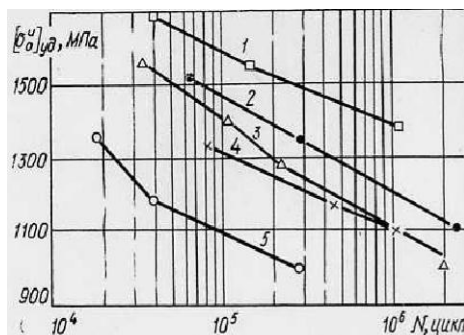


**Figure 1.2 Fatigue curves (Wöhler plots) for (1) WC20%Co, (2) WC15%Co, (3) WC25%Co, (4) WC8%Co, (5) WC6%Co (Loshak, 1984)**

The ratio of endurance limit ( $S_{e,5 \cdot 10^6}$ ) in cyclic bending and transverse rupture strength ( $R_{TZ}$ ) in static bending was equal to 0.7-0.8 (Miyake *et al.*, 1968) and 0.6 (Davies *et al.*, 1972). Such a great difference in the data obtained can be explained, first of all, by the imperfection of testing methods and techniques used. Usually, only 10-15 specimens of hardmetals were tested in the studies considered above and Wöhler's curves were plotted. Taking into account a considerable scatter of experimental data one can assume an obvious existence of a specific nature of hard metal fracture resulting from their production technology (Loshak *et al.*, 1972).

The two testing devices were designed for the high frequency cyclic loading - up to 200 Hz (Loshak, 1984). The loading scheme of both rigs was three-point bending with the zero-level of minimum stress. The first device was used in the so-called impact-bending tests and the other one was designed for bend cyclic loading.

More recent results on fatigue performance of cemented carbides were presented by Brookes (1982). Endurance limits of 600-850 MPa for  $10^8$  cycles for WC-Co (5...25wt%Co) were reported. These stress values lie at around 30% of the transverse rupture strengths. The results received by Schedler (1998) who determined endurance limits for similar materials in the range 30-40% of the  $R_{TZ}$  are in agreement with this.

The next loading scheme used by a research group from the University of Erlangen-Nurnberg to investigate fatigue performance is a new special cantilever-bending device developed for static, monotonic and cyclic alternating loading (Shleinkofer *et al.*, 1995).

A schematic representation of the apparatus used is shown in Figure 1.3, (a). Kennametal Hertel, F.R. Germany, produced the investigated hardmetals and cermets. The samples had the dimensions  $1.5 \times 2.5 \times 60$  mm for the tests at 22 Hz and  $3 \times 4 \times 90$  mm for the tests at 1Hz and 2Hz. The stress ratio of fully reversed bending load was  $R = -1$ . The surfaces of all samples were ground in a reproducible oscillating process.

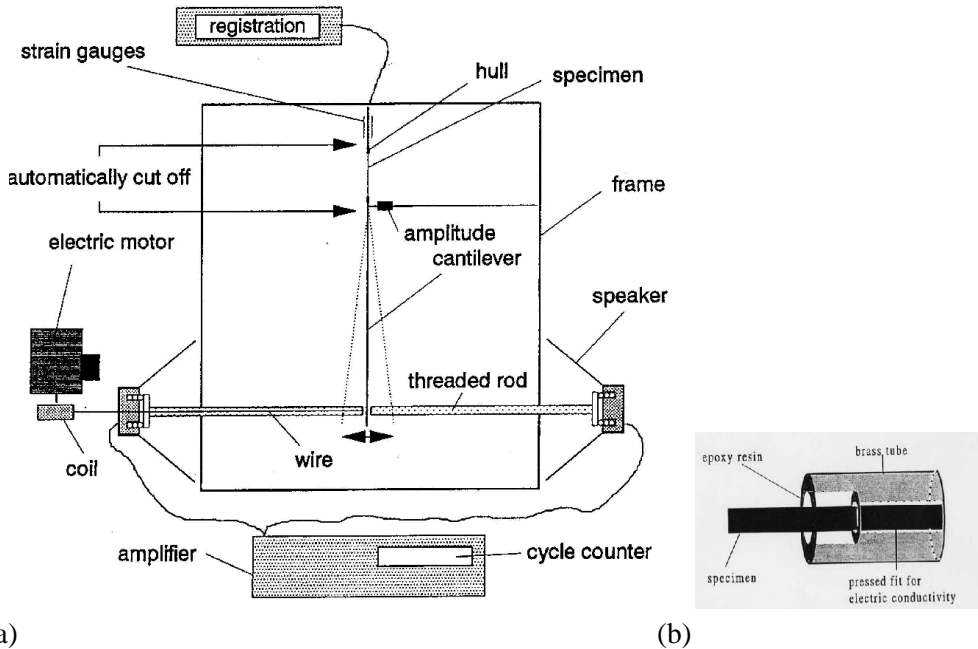


**Figure 1.3. The scheme of the testing rig used for three load conditions (a) and specimen preparation (b) for mechanical testing (Shleinkofer *et al.*, 1995) .**

The samples were embedded with an epoxy resin in brass tubes (Fig.1.3, b) in order to avoid stress concentration at the transition from sample to the fixing bracket. The compositions of the hard metals and cermets tested are given in Table 1.2.

The grain size of binder phase was in the range of 1  $\mu\text{m}$ . The sizes of carbide grains, containing Ti, Ta and Nb were in the range of 1.2 to 2.2  $\mu\text{m}$ . The characteristics of the fatigue performance of the alloys investigated are given in Table 1.3.

**Table 1.2 Compositions of hard metals and cermets (wt%) (Shleinkofer *et al.*, 1995)**

Compound	Hard metal A	Hard metal B	Hard metal C	Cermet A
WC	86.5	82.5	86.5	19.0
TiC	2.5	2.0	2.5	-
TiN	-	-	-	5.0
Ti(C,N)	-	-	43.0	30
(Ta,Nb)C	5.0	3.5	5.0	14
Mo <sub>2</sub> C	-	-	-	8.0
Co	6.0	12.0	4.0	10.0
Ni	-	-	2.0	6.0

The results showed that the resistance of hard metals and cermets against damage processes are significantly lower under cyclic loads than under static and monotonously increasing ones. The chemical composition and microstructure of alloy influences the resistance to failure.

**Table 1.3 Inert bending strength and endurance limits of hard metals A, B, C and cermet A (Shleinkofer *et al.*, 1996)**

Grade	Inert bending strength $S_{b,0}$ , (MPa)	Endurance limit $S_e \cdot 10^7$ , (MPa)
Hard metal A	2498	$\approx 960$
Hard metal B	2734	$\approx 900$
Hard metal C	2547	$\approx 615$
Cermet A	1835	$\approx 850$

When comparing hard metals and cermets, it became clear that the fatigue process occurs less strongly in cermet A. The slope of the dependency  $\sigma_{max} - \log N_f$  (Fig.1.4) is smaller for cermet A than in the results for hardmetals A, B and C. In other words, fatigue sensitivity of cermet is less than that of hard metals.

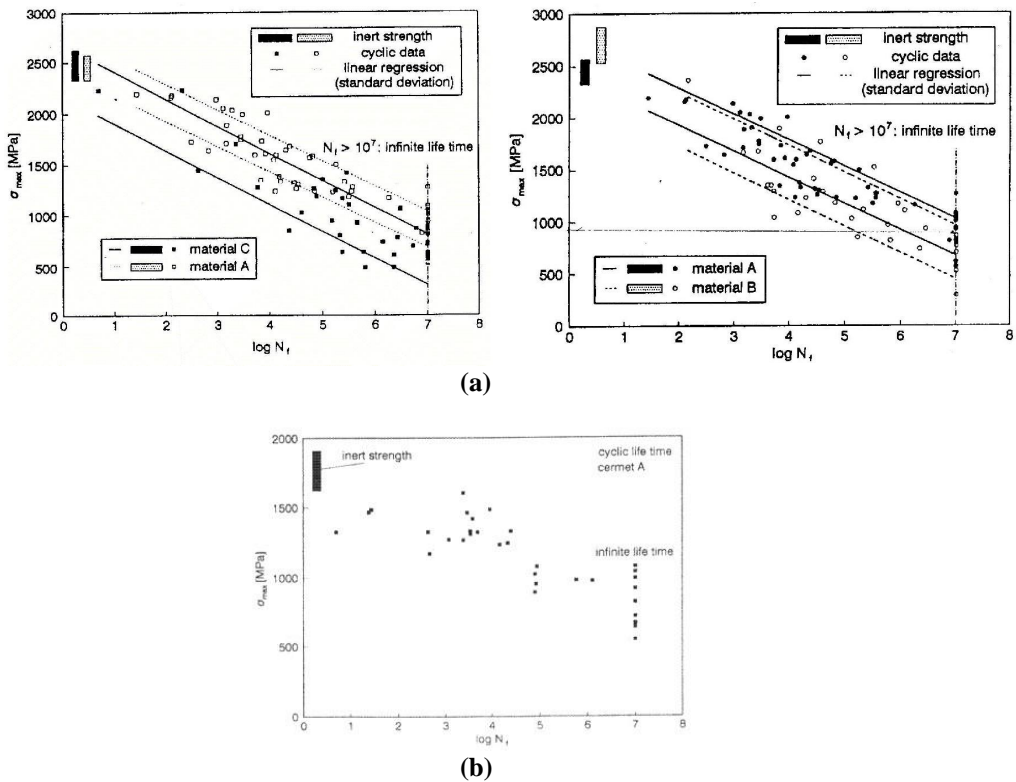


**Figure 1.4. Wöhler plots of the fatigue life for various types of hardmetals (a) and (b) cermet. (Shleinkofer *et al.*, 1996)**

The differences in the behaviour were clearer in the classical Wöhler plots (Figs.1.4, a and 1.4,b) and Wöhler plot (Fig.1.5) of relative stress amplitudes  $\sigma_{max}/S_{b,0}$  vs.  $\log N_f$ , where instead of  $\sigma_{max}$ , the ratio  $\sigma_{max}/S_{b,0}$  with the inert bending strength  $S_{b,0}$  of the materials are plotted. Higher slopes on this plot indicate higher accumulation of the

damage during the cyclic loading. It became clear from the plot that cermet A is superior in its behavior at higher  $N_f$  to the hardmetals. Another point to be highlighted on the plot in Figure 1.5: it was expected that one curve runs through 1 at  $\log N_f = 0$ . This is the case for hard metal A. The materials with higher binder content (hard metal B and cermet A) exhibit an intersection at a point below 1 for  $\log N_f = 0$ . It was assumed that this difference is caused by a damage mechanism, which occurs at a higher number of cycles in the materials with higher amounts of ductile binder phase. Such a process could be explained as a higher accumulated work hardening and different fatigue processes in the binder phases.

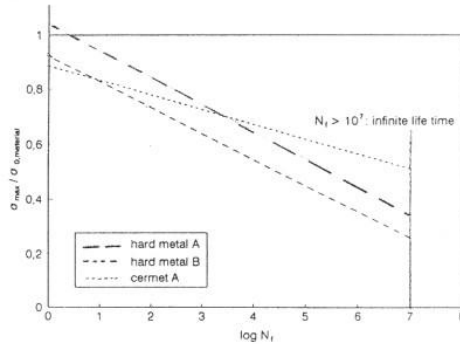
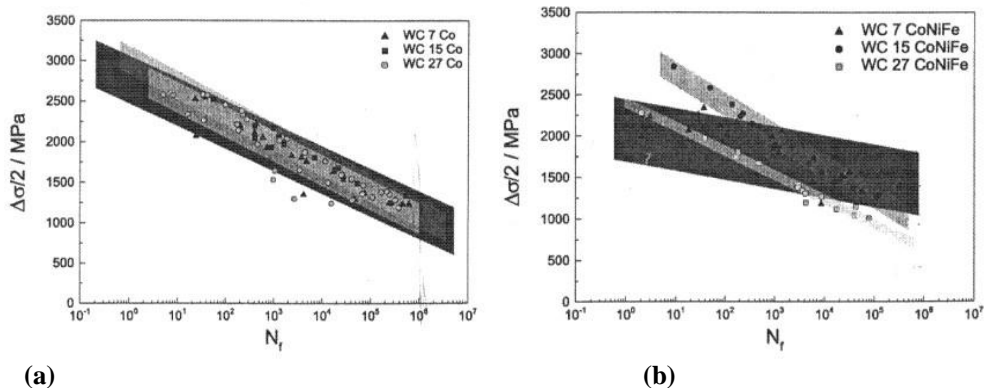


**Figure 1.5. Wöhler plots normalized by the inert bending strength (Shleinkofer et al., 1998)**

The investigation on the influence of binder content and composition on the fatigue performance of cemented carbides showed that the WC-Co grades (with 7, 15 and 27 wt% of Co) present little influence of the binder content on their fatigue behaviour due to the localization of damage in shear bands in the binder pools and the facilitated crack propagation in the transformed h.c.p.-binder phase or along stacking faults (Kursawe et al., 2001).



**(a) (b) Figure 1.6. Wöhler plots for WC-Co (a) and WC-CoNiFe (b) hardmetals (Kursawe et al., 2001)**

All these processes are responsible for the minor influence of the binder content on the fatigue behaviour of the WC-Co hard metals. The Wöhler plots in Figure 1.6, (a)

exhibit large scatter and almost identical slopes, which causes the Wöhler curves of all three materials to overlap. A decreasing width of the scatter band could be found with increasing binder content as the overall nature of the compound becomes more metallic. The composition CoNiFe-binder (with 7, 15 and 27 wt% Co) also exhibit reduced scatter with increasing binder content but the slopes of the Wöhler curves are different for each hard metal grade (Fig.1.6, b).

A clear influence of binder content on the fatigue behaviour of the WC-CoNiFe hard metals was found. This behaviour was explained with the absence of the binder phase transformation and the higher ductility of the CoNiFe alloy. The results of mechanical testing were confirmed by the results of the FEM simulation based on the plastic flow rules (Munz, *et al.*, 1989). Due to the higher ductility of the CoNiFe binder phase, the zones of plasticity are larger in the WC-CoNiFe hard metals than in the WC-Co ones. Data concerning the endurance limits measured are presented in Table 1.4.

**Table 1.4 Inert bending strength and endurance limits of hard metals WC-Co and WC-CoNiFe (Kursawe *et al.*, 2001)**

Grade	Inert bending strength $S_{b,0}$ , (MPa)	Endurance limit $S_{e, 10^6}$ , (MPa)
WC-7%Co	2840	≈1200
WC-15%Co	3178	≈1300
WC-27%Co	2887	≈1170
WC-7%CoNiFe	2859	≈1480
WC-15%CoNiFe	3122	≈980
WC-27%CoNiFe	2529	≈770

### 1.3 Fatigue crack growth behaviour of cemented carbides

While there have been several studies addressed to evaluate the fatigue performance of cemented carbides (mostly for WC-Co grades), only a few investigations have focused on the fatigue crack growth (FCG) behaviour of these materials (Hoenle *et al.*, 1998; Llanes *et al.*, 2000). Such limited information on FCG characteristics of hard metals is unfortunate, from the viewpoint of effective time-dependent (fatigue) property tailoring through microstructure control, once it is now well established that sub-critical growth of pre-existing flaws is the controlling stage in the fatigue failure of these materials. Several authors have studied the influence of microstructure and fatigue test parameters on the FCG behaviour of WC-Co cemented carbides has been studied, for relatively restricted sets of conditions. Although in such investigations a strong dependence of FCG rates on a particularly chosen fracture mechanics parameter (mainly the stress intensity factor range,  $\Delta K$ ) has been always found, none of the approaches applied for describing FCG kinetics in these materials allows a complete rationalization of the concomitant microstructural and testing effects observed (Ishihara *et al.*, 1999; Hirose *et al.*, 1997; Almond *et al.*, 1981 *etc.*)

An enhancement of FCG resistance with increasing binder content or carbide grain size was also reported (Fry *et al.*, 1983). The changes of latter correlating well with corresponding variations in fracture toughness. Knee and Plumbridge (1984) have also observed similar trends on microstructural effects, for two different load ratios. However, authors noticed such microstructural influence on FCG behaviour lessens with decreasing crack growth rates, to the limit of measuring crack propagation thresholds independent of both microstructure and toughness.

Hirose *et al.* (1997) discerned FCG kinetics to be significantly affected by both load ratio and WC grain size. This was found to be the case even when plotting crack growth data in terms of the effective stress intensity factor range,  $\Delta K_{eff}$  (after allowing for crack closure).

Finally, Ishihara *et al.* (1999) found a transition on the dominant fracture mechanics parameter for describing FCG kinetics, from  $K_{max}$ , the maximum stress intensity factor, to  $\Delta K$  with decreasing crack growth rates.

In the main report of results received by Llanes' *et al.* (2001) investigations, special attention was paid to analyse the experimental findings with respect to 1) relative dominance of static and cyclic failure modes during stable crack propagation; and 2) fatigue sensitivity, this parameter being defined as the ratio between the applied stress intensity factors corresponding to FCG threshold and the fracture toughness –  $K_{th}/K_{Ic}$ . The materials studied were plain WC-Co cemented carbides with different combinations of carbide grain size,  $d_{WC}$ , and cobalt volume fraction,  $V_{Co}$ . Values for cobalt binder thickness, or binder mean free path ( $\lambda_{Co}$ ) and carbide contiguity ( $C_{WC}$ ) were estimated by empirical relationships. The effect of load ratio  $R$  was evaluated from the FCG behaviour measured under  $R$ -values of 0.1, 0.4 and 0.7. Experimental results indicated that: 1) WC-Co cemented carbides are markedly sensitive to fatigue; and 2) their FCG rates exhibit an extremely large dependence on  $K_{max}$ .

Torres *et al.* (2000) conducted investigation and came to the agreement that, a more classical and conservative approach on the basis of fatigue limit and fatigue crack growth (FCG) threshold, i.e., from an infinite fatigue life viewpoint, appears to be more appropriate for brittle materials such as cemented carbides. This approach was implemented by simply defining critical flaw size under cyclic loading in terms of FCG threshold. Under this consideration, fatigue limit,  $S_e$ , was given by maximum stress ( $S_{max}$ ) resulting in the threshold intensity factor,  $K_{th}$ , of a small non-propagating crack emanating from a defect of critical size,  $2l_{cr}$ , according to relationships of type

$$S_e \propto \frac{K_{th}}{\sqrt{l_{cr}}}, \quad (1.1)$$

And then fatigue limit was estimated from Eq. (1.1), under assumption that strength-controlling flaws are the same, with respect to type, geometry, size and distribution under monotonic and cyclic loading

$$S_e = \left( \frac{K_{th}}{K_{Ic}} \right) R_{TZ}, \quad (1.2)$$

where  $R_{TZ}$  – is the transverse rupture strength. Such a correlation should not be considered as unexpected because it is implicit to the basis sustaining the whole analysis: (1) initiation of stable cracks growth as the controlling stage in the fatigue failure phenomena; and (2) similitude on the fatigue threshold behavior of large and small cracks (Torres *et al.*, 2000)

All presented correlations were in agreement with practical observations and results of conducted tests. The agreement between predicted and observed fatigue limits were described as excellent, with errors relative to the experimental values (Table 1.5) always lower than 10%, a finding that yields strong support to the FCG threshold-fatigue limit correlation proposed earlier.

**Table 1.5 Predicted and experimentally determined fatigue limit values, in term of maximum applied stress, for different load ratios for WC-10 wt% Co (Torres *et al.*, 2000)**

Load ratio $R$	Observed fatigue limit $S_e$ (MPa)	Predicted fatigue limit $S_e$ (MPa)
0.1	1827±92	1788
0.4	1783±70	1937
0.7	2112±70	2265

Furthermore, both fatigue sensitivity and relative prevalence of  $K_{max}$  over  $\Delta K$ , as the controlling fatigue mechanics parameter, were found to be significantly dependent upon the microstructure. As the mean binder free path increases (Fig.1.7), predominance of static over cyclic failure modes diminishes and a transition from a ceramic-like FCG behavior to a metallic-like one occurs (conversely in relation to contiguity).

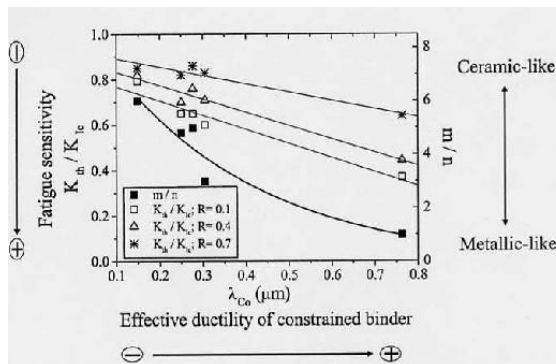


**Figure 1.7. Fatigue sensitivity – microstructure relationship for WC-Co hardmetals. ( $m/n$  ratio from Paris-Erdogan equation) (Llanes *et al.*, 2002)**

The trade-off between fracture toughness and FCG resistance becomes more pronounced with increasing binder content and carbide grain size. The observed

behavior is attributed to the effective low ductility of the constrained binder and its compromising role as the toughening and fatigue-susceptible agent in hard metals, the latter on the basis that cyclic loading degrades or inhibits toughening mechanisms operative under monotonic loading, i.e. crack bridging and constrained plastic stretching (Llanes *et al.*, 2002).

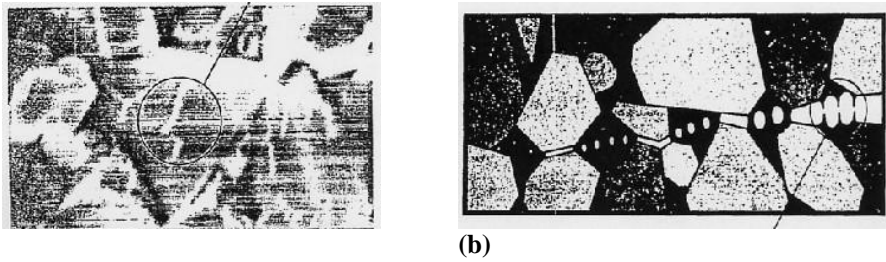
#### 1.4 Microstructural aspects and fractography of fatigue crack growth in cemented carbides

Schlienkofer *et al.*, (1996) observed a stable crack propagation of small natural cracks during fatigue loading. The compositions of cemented carbides subjected to the investigation given in Table 1.6.

**Table 1.6 Compositions (wt.%) of the hard metal and cermets subjected to microstructural investigations (Schlienkofer *et al.*, 1996)**

Compound	Hard metal	Cermet A	Cermet B
WC	86.5	19.0	-
TiC/TiN	2.5	43.0	-
(Ta, Nb)C	5.0	14.0	-
Mo <sub>2</sub> C	-	8.0	-
(WTiTa NbMo)(C,N)	-	-	84.0
Co	6.0	10.0	10.0
Ni	-	6.0	6.0

The cracks propagated predominantly in the ductile Co-binder phase, which in itself undergoes a strong plastic deformation, especially in the ligaments formed behind the crack tip (Fig.1.8). The ligament zone has a great influence on the mechanical behavior of the WC-based hard metals. TEM investigations showed that the martensitic phase transformation from f.c.p. to the h.c.p. structure occurs in the Co-binder ligaments. This transformation is a result of a high level of accumulated deformations at high cyclic stresses during fatigue. It was observed to a much smaller extent under static or monotonic loads. A consequence of this transformation is that the ductility of the ligaments behind the crack tip is reduced, thereby leading to a strong reduction of the crack tip shielding effect. It is interesting that the process described above is opposite to the normal observation of deformation-induced transformation toughening of materials. More detailed investigations of the microstructural behavior of binder phase of cermets A and B showed that the dislocation network was observed in the phase boundary between core-(Ti(C,N)) and rim-((TiWTa Nb)(C,N)). The microstructure of the core and the rim developed during sintering has no or only a very small lattice misfit between two phases.



**(a)** **Figure 1.8. SEM image of the fracture surface (a) with binder ligaments of the hardmetal, which failed under monotonic loads and schematic representation of the multiligament zone (b) (Sigl, 1996)**

The microstructure of the (Co,Ni)-binder was the same for two cermets. Considering that investigations of the mechanical response of cermet B lead to higher values of the bending strengths than cermet A one under monotonically increasing loads, the different core-rim microstructures of cermets were assumed to be responsible for this effect. However, the binder phase was the same in both cermets, so it was expected approximately the same fatigue performance. The assumption was based on the result of the SEM investigations and results done earlier (Sigl, 1996; Exner *et al.*, 2001). Phase transformation of (Co,Ni)-binder was not observed in the cermets.

The quantitative fractography has been used as a tool in the study of cermets fracture concerning stable and unstable crack propagation (Torres *et al.*, 2001). A series of WC-Co grades were selected with 10 wt.% binder content and a coarse (2.2  $\mu\text{m}$ )/ fine (1.5 $\mu\text{m}$ ) mean carbide grain size. Three-point bending tests (span with 28 mm) with prismatic samples (32 $\times$ 6 $\times$ 2 mm) were used. A Chevron notch cut with a 100  $\mu\text{m}$  diamond blade made it possible to proceed from stable to unstable crack growth in each specimen. A function generator allowed to load the specimen with a preset rate of bending or, alternatively, with a preset loading rate. In this way, fracture surfaces produced by four different conditions of crack growth were available for WC-Co 10wt.% alloy. Fractographic examination did not allow discerning, in agreement with previous work (Almond *et al.*, 1980; Fry *et al.*, 1983; Knee *et al.*, 1984)

An instrumented stereometer (Exner *et al.*, 2001) was used to measure the lengths and the angles of fracture facets along profiles in the direction of crack propagation. The results obtained from the stereophotogrammetry of fracture surfaces present a univocal proof that at room temperature stable and unstable cracks take the same path through the microstructure. Under sub-critical conditions, the crack proceeds in jumps over short distances with high velocity and stops for some time until at progressing crack opening the stress intensity reached the local critical value again. However, rest lines as observed in fatigue failure have not been detected. This was ascribed to the fact that the fracture surfaces were too irregular and the jumps were short (e.g., one or a few grain dimensions) and frequent (Chermant *et al.*, 2001). Stable and unstable cracks in brittle materials proceed with about the same velocity: unstable cracks producing catastrophic failure proceed in a single jump while stable cracks proceed in small ones. The frequency and step width of the jumps vary locally as set by the loading

conditions and local microstructure. If, however, a time-dependent mechanism is involved in the fracture progress (low loading rates or temperature increase), the crack may change its path (from predominantly trans-crystalline to partially inter-crystalline), which was reflected in the geometry of the fracture surfaces.

The work of Sigl (1996) resulted in a complete quantitative description of the nature of fracture in cemented carbides culminating in a precise quantitative correlation between fracture toughness and microstructure of WC-Co alloys in the technically relevant range of Co-contents and carbide grain size.

### 1.5 Mechanical and tribological behaviour of cemented carbides

It is evident that blanking dies are heavily loaded tribosystems, which are characterised by very high wear rates in very serious forms of wear – adhesion and abrasive. A characteristic feature of wear process is that forces act on asperities repeatedly. As sliding continues damage accumulates in the material, which leads to eventual fracture. This is nothing but fatigue failure. It seems clear, therefore, that the property representing the resistance of materials to wear is the resistance to fatigue failure, no matter what model is employed. Therefore, the reliability of hardmetals in metal forming operations depends, first of all, on their resistance to fracture, caused by alternating loading (under combined Mode I and II conditions) (Smith, 1980).

The complexity of the wear processes is understandable if take into consideration fact that many variables are involved, including hardness, toughness, modulus of elasticity, yield strength, structure and composition, as well as geometry, contact pressure, temperature, state of stress, coefficient of friction, surface finish and etc.

Reshetnyak (Klaasen) et al., (1998) presented the relationship adhesive wear resistance – hardness, (Fig.1.9, a) which shows that structure sensitivity of hardmetals in adhesive wear conditions is much higher than that of in the abrasive –erosion wear.

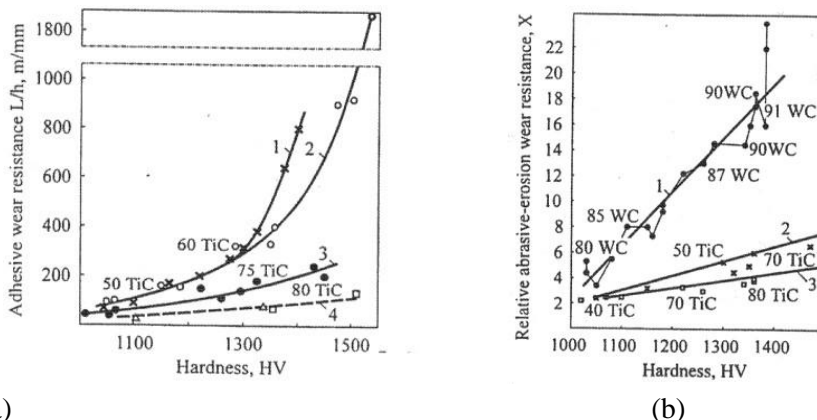


**Figure 1.9. (a) - Adhesive wear resistance vs. Vickers hardness: WC-Co (1) and TiC-base cermet, martensite (2), austenite (3), pearlite (4) binder. (b) – Relative abrasive-erosion wear resistance vs. Vickers hardness: WC-Co (1), and TiC-base cermet (2- martensite binder, 3- alloys with austenite binder) (Reshetnyak et al., 1998)**

At equal level of hardness the differences in the resistance to erosion of TiC-base cermets with different binder does not exceed 100% (Fig1.9, b). The differences in adhesive wear resistance between TiC-base cermets with different binder compositions and structure increases with increasing of carbide content and may differ at equal level of hardness up to 10 times. It was noted also, that unlike in abrasive-erosion wear difference in adhesive wear resistance between different families of cemented carbides (WC- and TiC-base) is at the same level of hardness less than that between TiC-base cermets with different structure of binder.

High sensitivity to structure also was highlighted from relationships presented in Figure 1.10. Decrease in grain size induces a decrease in the adhesive wear parameter  $h$  from 2.5 to more than 5 times depending on carbide content in the alloy. The influence of carbide grain size on adhesive wear depends on the binder content in alloy stronger than that in the case of abrasive-erosion wear. The adhesive wear resistance impairment with increasing of the mean carbide grain size  $d_{WC}$  is the greater the lower carbide fraction of the cemented carbides (Reshetnyak *et al.*, 1998).

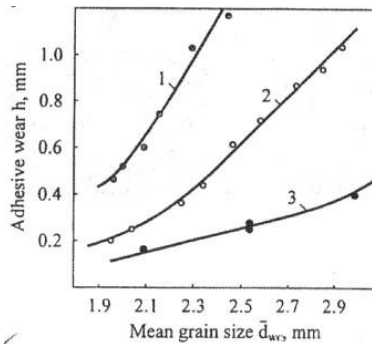


**Figure 1.10. Adhesive wear vs. mean grain size of carbide phase in WC-Co hardmetals (1- 20% Co, 2- 15% Co, 3- 10% Co) (Reshetnyak (Klaasen) *et al.*, 1998)**

Certain peculiarities of adhesive and abrasive-erosion wear processes were highlighted. Failure mechanism of hardmetals during abrasive and adhesive wear allowed to state that there is a similarity between both phenomena: the failure of material is a two-step process. The failure starts with formation of pre-conditions – elastic-plastic penetration of abrasive particle into material during abrasion and local plastic strain resulting in formation of physical contact (juvenile surfaces) between wearing surfaces during adhesive wear. In the second step the process finishes with removal of material by micro cutting in abrasive wear and by extraction of material during adhesive one. Therefore, it was concluded that under abrasive wear conditions wear resistance depends mainly on two characteristics – resistance to penetration or elastic-plastic strain and resistance to cutting or resistance to shear stress (Mode II fracture), on their combined effect. Regarding the similarity of stress states in Mode II fracture and compression fracture compression strength  $R_{cm}$  has been offered as additional to hardness characteristic. Clear correlation between relative wear resistance  $X$  and the product  $HV \cdot R_{cm}$  for both cemented carbides classes have been obtained (Reshetnyak (Klaasen) *et al.*, 1994).

The higher abrasive-erosion wear resistance of WC-base hardmetals was related first their higher modulus of elasticity. The latter as an even more important characteristic for evaluation of abrasive wear than hardness. A combined factor – the product  $E^m R^{n_{c0.1}}$  suggested for abrasive-erosion wear evaluation. A good applicability of relationship X vs.  $E^m R^{n_{c0.1}}$  was supposed to be an effective for metallic alloys as well. Analysis of obtained results allowed us to conclude that TiC-base cemented carbides are competitive materials in adhesive wear conditions due to their high resistance to local plastic deformation (Reshetnyak (Klaasen) *et al.*, 1998).

The applied toughness was a novel empirical characteristic suggested by Reshetnyak (Klaasen) and Kübarsepp (1998). It represents the product  $(\varepsilon_p \cdot R_{TZ})$  of two parameters ultimate plastic strain in uniaxial compression ( $\varepsilon_p$ ) and transverse rupture strength ( $R_{TZ}$ ). In essence, the applied toughness describes fracture energy that a carbide composite is able to absorb by local plastic strain without crack propagation. It embraces properties determined in bending and uniaxial compression tests. The use of such combination was justified by the fact that the stress state of tool in blanking service conditions is an intermediate between bending and uniaxial compression states (Fox-Rabinovich, 1994).

### 1.6 Statistical consideration of cemented carbides fatigue performance

The two main principles influencing reliability of brittle materials are the statistical nature of component strength and its time-dependent degradation under stress. This statistical aspect derives from the fact that the strength is limited by the distribution of the most severe defects in the component (i.e., the strength-determining flaws). Because flaws are generated both by processing and by in-service use and handling, the initial strength is described by a statistical distribution rather than by a fixed value. Therefore, an important step in the lifetime prediction process must be a statistical analysis of the experimental results.

In assessing the reliability of brittle composites, Weibull distribution has proved to be an useful and versatile means to describe statistical strength and fatigue life data (Weibull, 1939). The failure probability is given by

$$F = 1 - F_s = 1 - \exp \left[ - \left( \frac{\sigma_f}{\sigma_{f,0}} \right)^{m_w} \right] \quad (2.3)$$

where  $\sigma_{f,0}$  - mean inert strength,  $\sigma_f$  - inert strength of  $i$ -sample and  $m_w$  – Weibull modulus for static loading.

For the cyclic load conditions, Weibull distribution is given by

$$F = 1 - \exp \left[ \left( \frac{N_f}{N_{f,0}} \right)^{m_c} \right] \quad (2.4)$$

where  $N_f$  - number of cycles to failure,  $N_{f,o}$  - the mean cycle number,  $m_c$  – Weibull modulus for cyclic alternating loads. The failure probability  $F$  is defined for both cases as

$$F = \frac{(i - 0.5)}{n} \tag{2.5}$$

with the sort index  $i$  and  $n$  the number of specimens (Weibull, 1941).

The evaluation of the parameters  $\sigma_0$ ,  $m_i$ ,  $N_{f,o}$ ,  $m_c$  (the Weibull statistics) is usually carried out using the maximum likelihood method (ENV 843-5:1996). It is the method of numerical procedure, which leads to more accurate results of the Weibull parameters compared to the evaluation directly out of the Weibull plot by using geometric methods or linear regression. There are many theories, which are based on the Weibull “weakest link” ideas. However, the difference between the predictions and data obtained for many stress systems is considerable. The number of inner defects of material is characterized by parameter  $m$ , which is also known as homogeneity module. Due to the scatter in the failure loads and the inevitable experimental errors, it is always difficult to decide which theory is the most appropriate.

Loshak et al. (1981) obtained Weibull parameters data for various loading conditions. Data are presented in Table 1.6. It should be noted that parameters  $m$  and  $\sigma_0$  are different for various hard metal-grades and testing procedures. It is usually explained by the differences of inner (bulk) and outer (surface) flaw distribution. Weibull modulus is related to the rate at which flaws become critical with the stress compared to the number of flaws that are already critical (Danzer, 1992).

**Table 1.6 Weibull statistics obtained for hard metals tested by different loading schemes (Loshak, 1981)**

Loading scheme	H6 (WC-Co 6%)		H15 (WC-Co15%)		H25 (WC-Co25%)	
	$m$	$\sigma_0$ , MPa	$m$	$\sigma_0$ , MPa	$m$	$\sigma_0$ , MPa
Tension	9	1740	9	2390	9	2700
Compression	13	6780	15	4900	18	4460
3 Point-Bending	14	2150	12	2970	11	3100
4 Point-Bending	10	2260	10	3170	11	3110
Cyclic 3Point-Bending	7	1650	8	2060	9	2240
Static Torsion	8	910	8	2050	8	2430

The overall objective of incorporating probabilistic analysis into fatigue design is to ensure that a low probability exists for a combination of higher than average cyclic stress amplitude and a lower than average fatigue endurance limit (or stress amplitude

at a fixed life) to cause failure. In practical design involving the stress-based approach to total fatigue life, however, an endurance limit is first established on the basis of experiments conducted on carefully prepared smooth test specimens. This limit is then lowered by applying modifying factors to account for such effects as surface finish, size effects and constraints, temperature, stress corrosion and numerous unknown effects (White *et al.*, 1999).

The studies concerning Weibull statistics determination summarized by Shleinkofer *et al.* (1998) showed that hardmetal H12 has a higher value of mean inert strength and all its data in Weibull distribution lay significantly higher as compared with inert strengths. Therefore, the knowledge of the behaviour of the binder phase is of great importance. The results are presented in Table 1.7.

**Table 1.7 Weibull statistics of the tests under monotonously increasing and cyclic loads in cantilever bending (Schleinkofer *et al.*, 1998)**

Weibull parameter	H6 (WC6%Co)	H12 (WC12%Co)	H6CoNi (WC6%CoNi)	C16 CoNi(Ti(C,N)- 16%CoNi)
Monot. $m$	39	23	28	26
Monot. $\sigma_0$ (MPa)	2498	2734	2547	1835
Cyclic $m$ (at $\sigma_{\max}=1200$ MPa)	2.27	1.49	-	-
Cyclic $N_{f,0}$ , cycles (at $\sigma_{\max}=1000$ MPa)	350000	550000	-	-

The results from the tests of properties measurement, proper estimation of statistical parameters of data distribution are usually combined to give a lifetime prediction. However, there is still no way to estimate how statistically significant the lifetime prediction is. To obtain as much information as possible from the lifetime prediction model, it is necessary to estimate the confidence limits associated with the prediction. A special technique is to be used to evaluate the lifetime adequately at whatever confidence level is desired (White *et al.*, 1999).

## 1.7 Objectives and strategies

WC-base cobalt-bonded hardmetals are the most widely used hardmetals because of their excellent strength-wear resistance combination. Among tungsten-free cemented carbides TiC-based ones, cemented with iron, nickel and molybdenum are utilized today to a minor extent only. However, high hardness, chemical inertness, respectable strength and fracture toughness, combined with relatively low production costs, make titanium carbide-base materials one of the widely used wear resistance composites. Recent improvements in materials processing which have resulted in improvement material reliability have created a renewed interest in TiC-base cermets. It is important to note that until now there is no complete understanding of the material behavior under complex service conditions where all the phases of heterogeneous cemented carbide are subjected to various type of loading.

Considering the details of previous research in a field of durability of tungsten-free cemented carbides the obvious need to enlarge the knowledge of materials' behavior under cyclic loading conditions occurs.

The objective of the present research was to clarify the fatigue phenomena of major grades of cemented carbides and quantify their fatigue characteristics under a constant amplitude cyclic loading. It was important also to connect main mechanical characteristics of materials with their fatigue durability and to assess the microstructural features of fatigue fracture.

To obtain such data the following strategies were used:

- the accelerated fatigue testing procedure for preliminary assessment of constitutive behaviour (designed and applied);
- the standard fatigue testing (in three-point bending);
- wear tests under adhesive and abrasive-erosion conditions (conducted at ambient temperature);
- the statistical strength and Weibull modulus (calculated and assessed);
- the service conditions testing procedure (blanking operation of sheet metal);
- the fractography and XRD investigation (of fractured and non-fractured specimens);
- the estimation of fatigue strength of heterogeneous materials containing defects (Murakami approach).

## 2 EXPERIMENTAL PROGRAM

Materials' testing to obtain  $S-N$  curves is a widespread practice. The need for this approach arises from a scatter of fatigue data. The resulting data and curves are widely available in the literature, including various handbooks. An understanding of the basis of these tests is useful effectively to employ their results for engineering purposes. It is known that collection of fatigue tests data is a time-consuming issue, which results in additional complexity in evaluation of fatigue strength. Statistical analysis of fatigue data permits the average  $S-N$  curve to be established for various probabilities of failure (Dowling, 1998). But still there are errors of 100% and more are possible. Small changes in the composition, design and processing of parts also can have a considerable influence on fatigue strength and scatter.

### 2.1 Materials

#### 1.2.1 Materials characterization

For the investigation of the fatigue behaviour two WC-Co hardmetals and three TiC-base cermets were submitted to static and cyclic loading tests at ambient temperature. High wear resistance combined with high values of strength and toughness is features of these materials. They have found especially wide application in producing tools for plastic working of metals, in particular, for sheet metal forming (stamping and blanking dies). The Laboratory of Powder Metallurgy of Tallinn University of Technology produced the investigated samples. The set of mechanical properties of the TiC-based cermets selected in correspondence with those of WC-based ones were used in blanking operations: hardness  $HRA \geq 87$ , transverse rupture strength  $R_{TZ} \geq 2.1$  GPa. Mechanical properties and compositions of tested cemented carbides (at ambient temperature) are given in Table 2.1.

#### 1.2.2 Specimen preparation

All materials investigated were produced through conventional press and sinter powder metallurgy. According to ASTM B406, the cemented carbide specimens were prepared to the following dimensions (width  $\times$  height  $\times$  length, respectively) WC-Co grades  $5.0 \pm 0.3 \times 5.0 \pm 0.3 \times 19$  (mm<sup>3</sup>), TiC-base -  $5.0 \pm 0.3 \times 5.0 \pm 0.3 \times 16$  (mm<sup>3</sup>). Specimens were ground to a surface finish of  $\approx 15$   $\mu$ m for WC-Co hardmetals and  $\approx 25$   $\mu$ m for TiC-base cermets on four sides. Opposite ground faces were parallel within 0.03 mm.

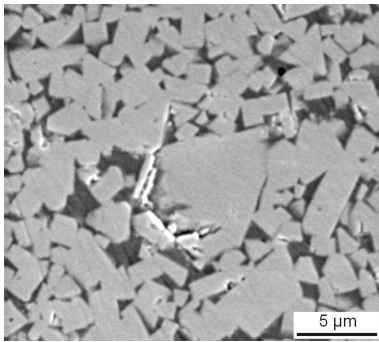
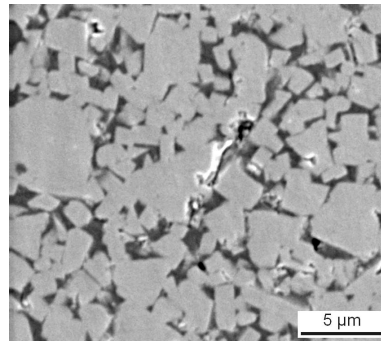
Careful grinding techniques were used to prevent various forms of surface cracking (flaws), which are able degrade the measured strength. The four edges of the specimen representing the intersection of the ground faces were chamfered to a maximum of 0.4 mm by 45°.

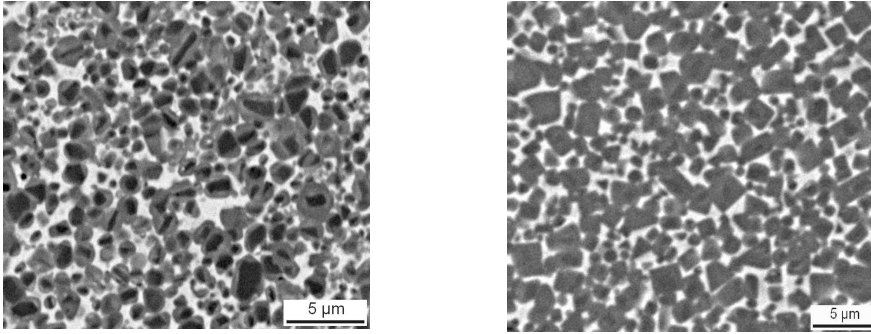
**Table 2.1. General data and mechanical properties of materials tested**

Tested materials	H10	H15	T30	T60/8	T70/14
WC content, wt%	90	85	-	-	-
TiC content, wt%	-	-	70	60	70
Binder composition and structure	Co	Co	Ni/Mo (2:1)	Fe/8wt% Ni martensite	Fe/14wt%Ni austenite
Carbide average grain size, $d_g$ ( $\mu\text{m}$ )	2.0	2.1	2.0	2.2	2.0-2.4
Hardness, <i>HRA</i>	87.5	87.5	88.5	87.5	88.5
Transverse rupture strength, $R_{TZ}$ (GPa)	2.2	2.7	1.6	2.2	2.4
Proof strength $R_{Co.1}$ (GPa)	3.0	2.3	2.1	2.4	2.2
Young's modulus, $E$ (GPa)	670	600	395	-	410
Ultimate plastic strain, $\epsilon$ (%)	1.1	1.5	0.8	1.6	1.8

### 1.2.3 Microstructural features

The microstructures of the tested WC-10wt%Co and WC-15wt%Co hardmetals are shown in Figure 2.1, (a) and (b). The cobalt binder is dark, while tungsten carbide grains are lighter. The shape of carbide grains is angular. The shape of TiC grains is rounded with no sharp corners. The Microstructure of TiC-base cermets is presented in Figure 2.1 (c) and (d), respectively.

**(a)****(b)**



(c) (d)  
**Figure 2.1. Microstructure of the investigated WC-based hardmetals (a) H10, (b) H15 and TiC-based cermets (c) T30 and (d) T70/14**

The titanium carbide grains are dark and the binder is lighter. Two different types of TiC-base cermets were subjected to investigation – (Ni/Mo)-bonded and steel-bonded. Austenitic and martensitic steel was formed during sintering in TiC-steel bonded cermets due to various contents of Ni in the Fe/Ni binder compositions (Table 2.1).

## 2.2 Accelerated fatigue testing

An accelerated fatigue testing suggested is a procedure [Appendix B, I], based on the idea of evaluating the relationship between stresses and the number of cycles by special staircase loading schemes. As a result, the constitutive equations in the exponential form were obtained. Accelerated tests may be used for different structural materials for which the time properties obey the exponential law [Appendix B, I, Eq.1]. The aim was to accelerate the time-consuming fatigue testing and preliminary to assess the fatigue performance of new materials. On the grounds of the basic theory of thermal activation processes N. Zhurkov (1965) have received the durability in the following form

$$t = \nu \cdot e^{\frac{U - \gamma\sigma}{KT}}, \quad (2.1)$$

where  $\nu$  is the frequency fluctuation factor, which is close by its value to the period of free thermal molecular oscillation ( $10^{-23}$  to  $10^{-12}$  s). The stress action reduces the energy of activation from  $U$  to  $U - \gamma\sigma$ , where  $\gamma$  is the factor dependent on the activation volume, i.e., on the structure of the material. The product  $\gamma\sigma$  corresponds to the work of the stress at the molecular bonds in the initial structure;  $K$  is Boltzmann's factor;  $T$  is the absolute temperature (Baily, 1951).

At the constant temperature Eq. (2.1) can be used for various materials rewritten as follows:

$$t = A \cdot e^{-\alpha\sigma}, \quad (2.2)$$

where  $A$  and  $\alpha$  are constant factors dependent on the temperature and the mechanical properties of the material. The exponential dependence of the durability  $t$  on the stress

$\sigma$  is well proved for the materials such as plastics, aluminium alloys, and hardmetals: WC- and TiC-base sintered powder materials. Eq. (2.2) can also be used in the form

$$N = A \cdot e^{-\alpha\sigma}, \quad (2.3)$$

where  $N$  is a number of stress cycles until fracture. To determine material constants  $A$  and  $\alpha$ , it is necessary to conduct two series of tests on condition that the values of the stresses  $\sigma_0$  and  $\Delta\sigma$  will be equal for both series, but the number of cycles (or time) in each step for the first series is equal to  $\Delta N_1$  and for the second series is equal to  $\Delta N_2$  [Appendix B, I, Fig.1].

### Results

The two constitutive exponential equations were obtained for cemented carbides for a preliminary assessment of their fatigue behaviour.

For WC-15wt% Co (H15) alloy:

$$N = 1.954 \cdot 10^7 \cdot e^{-0.0014\sigma} \quad (2.4)$$

And for TiC-30wt%FeNi (T70/14) alloy:

$$N = 1.436 \cdot 10^7 \cdot e^{-0.0009\sigma} \quad (2.5)$$

The important constitutive material constants  $A$  and  $\alpha$  were calculated using an accelerated testing approach. The curves obtained from testing can be used as prediction curves for the assessment of lower bands of fatigue limits for these two particular cemented carbides.

Fatigue constitutive curves obtained from accelerated testing are presented in Figure 2.2.

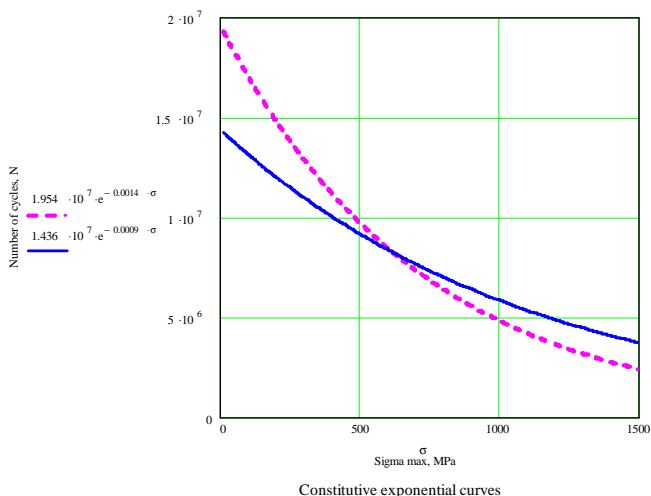


**Figure 2.2. Fatigue constitutive curves for H15 (dash line) and T70/14 (solid line) alloys received by the accelerated testing procedure**

### 2.3 Wear testing

There were three major wear testing schemes used: adhesive, abrasive-erosion and sliding wear. Wear tests were complemented by functional tests – service conditions durability tests [Appendix B, III].

A special method was elaborated for adhesive wear testing. The essence of the method is turning of mild steel (170HV) at low cutting speed, in which adhesion phenomena predominate. The wear rate was determined as the height  $h$  of the wear land at the tool (specimen) tip after a specific length of the cutting path  $L$ . The adhesive wear resistance was determined as the length of the cutting path when the height of the wear land achieved the critical value of 1 mm. The critical height of the wear land corresponded to the onset of the accelerated wear [Appendix B, III, Fig.3]. Confidence interval of the wear resistance did not exceed 10% when the number of test specimens was at least three.

Abrasive-erosion tests were conducted on a centrifugal accelerator [Appendix B, III]. The conditions were as follows: abrasive-quartz sand with particle size  $0.1\pm 0.2$  mm, jet velocity  $80\text{ m}\cdot\text{s}^{-1}$  and attack angle  $30^\circ$ . The abrasive-erosion rate was determined as specific volume wear ( $\text{mm}^3$ ) corresponding to 1 kg of abrasive. The relative wear resistance  $X$  was determined as the ratio of the wear rate of the studied alloy. Four test specimens were analysed and the wear rate confidence interval 10 % with the probability factor of 95 %.

Sliding wear tests were performed in accordance with the ASTM standard B611-85, without abrasive at a loading 40N and wear path length equal to 4000m. The volumetric wear rate was calculated as  $\Delta V = \Delta m / \rho$ , where  $\Delta m$  is the average mass loss and  $\rho$  is the density of the alloy.

### Results

In terms of abrasive-erosion wear resistance TiC-base cermets, as expected, have a considerable disadvantage over the WC-base hardmetal. The results of the experimental investigation demonstrate the superiority of titanium carbide base cermets over the WC-base hardmetal from point of view of adhesive wear resistance point of view. This confirms that the adhesive wear resistance of carbide composites depends primarily on the properties of the binder and less on those of the carbide phase. In its turn, the abrasive wear resistance depends, in contrast to adhesive wear processes, on the properties of carbide phase: its strength and rigidity. In general, it may be stated that between the blanking performance of materials investigated and their adhesive wear resistance a fair correlation exists [Appendix B, III, Fig.4]. The nature of failure and the fractured surfaces in adhesion testing and in the service condition testing were similar [Appendix B, III, Fig. 5]. After removal of the binder, the worn areas of the subsurface act as failure initiating stress concentrators inducing acceleration of wear process. In the last step, the removed carbide particles act as abrasive particles. The investigation of worn surfaces near the cutting edges of blanking tools by SEM exposed some differences in the micro-mechanism of wear

[Appendix B, III, Fig 7 and 8]. The formation of the local microfailure results in the microchipping of cutting edges during blanking. Microchipping of cutting edges causes an increase in shearing forces (Mode II cracking), which results in the acceleration of the side wear.

## 2.4 Fatigue testing

In order to evaluate the fatigue data and the damage processes under cyclic load conditions the behaviour of materials under monotonic loads has to be determined. The result obtained from monotonic testing was an inert bending strength in three-point bending loading ( $R_{TZO}$ ), which was further used for cyclic stress levels selection in cyclic loading [Appendix A, Fig.A1]. Twelve specimens of each grade were subjected to monotonic loading. The same three-point bending procedure was used for fatigue data accumulation. The procedure used is complies with ISO 3327 (ASTM B406). The investigations were carried out on the dynamic and fatigue test system INSTRON 8516. The test apparatus was automatically controlled by a Windows microcomputer-based system. Data processing and registering was made with the Max v4.2 software.

The controlled parameters were: 1) cyclic loading parameters (loading scheme with loading amplitudes), 2) the loading frequency and 3) the displacement of the zero position of specimen. The fatigue limits were defined for lifetimes as long as  $10^7$  cycles. The schematic representation of the loading history of mechanical tests is shown in Figure 2.3. The frequencies of cyclic loading were equal to 1 and 22 Hz. The velocity of the load applied did not exceed  $1 \text{ kNs}^{-1}$ . The fracture occurred around the middle of the specimen within one third of the span between the supporting cylinders on the tension side of the specimen. The maximum applied cyclic stress was equal to 90% of  $R_{TZO}$ . The stress ratio  $R$  was equal to 0 for all cyclic tests.

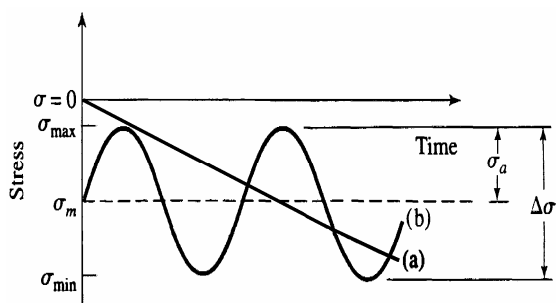


**Figure 2.3. Schematic representation of the load history in bending: under monotonic (a) and cyclic (b)**

## Results

The resistance of materials tested to the damage processes under cyclic loading is much lower than under static monotonic loading. The different slopes of the regression scatter bounds express the different fatigue sensitivity of the materials. It is

obvious that the grades with lower fatigue sensitivity are more suitable for application under service conditions where the cyclic loading takes place. Higher slopes in the plots indicate a higher degree of accumulation of damage during the cyclic loading. Thus, the cermet T70/14 is superior in its behaviour at a higher number of cycles. The fatigue testing data are presented in Figure A4 in Appendix A.

The estimated endurance limits, Weibull statistics of monotonic and cyclic loading histories are presented in Table 2.1.

**Table 2.1. Endurance limits and Weibull parameters for monotonic and cyclic loading**

Grade	Endurance limit $S_e$ , (GPa)	Weibull parameter for monotonic loading (MLE) $m_0$ and $S_{b0}$ (MPa)		Weibull parameters for cyclic loading $m_c$ and $N_{f0}$	
H10	1.23	18.7	2.3	0.42	$\approx 440000$
H15	1.56	14.5	2.7	0.81	$\approx 560000$
T60/8	0.62	10.2	2.2	0.47	$\approx 320000$
T70/14	1.41	13.6	2.4	0.64	$\approx 670000$
T30	0.51*	10.8	1.8	0.37*	$\approx 240000^*$

\*on the basis of  $10^5$  cycles

The evaluations of Weibull parameters were carried out using maximum likelihood estimation (MLE) method. The determined parameters are equated in accordance with DIN 51110. Considerable scatter of data for hardmetal H10 is explained by the lower content of binder, which causes the higher degree of heterogeneity of the composite. Wöhler plots  $S_{max}$  vs.  $\text{Log}N$  (number of cycles until failure) is shown in Figure A1 [Appendix A]. The fatigue strength of carbide composites varies in proportion to their toughness characteristics. It has been emphasized that the fatigue strength-applied toughness relation is more accurate than that of fatigue strength-stress intensity factor one [Appendix B, IV, Figs.3 and 4].

**Table 2.2. Threshold characteristics of the materials investigated**

Grade	Fracture toughness $K_{IC}$ , $\text{MPa}\cdot\text{m}^{-1/2}$	Threshold stress intensity factor $K_{th}$ , $\text{MPa}\cdot\text{m}^{-1/2}$		Endurance limit $S_e$ , GPa	
		Previous work	Present work	Previous work	Present work
H10	14.0	6.8	8.9	1.3	1.23
H15	17.0	6.3	9.7	1.5	1.56
T30	9.5	-	6.4	0.4*	0.5*
T70/14	18.0	-	11.9	1.2	1.41

\*on the basis of  $10^5$  cycles

Improvement of fatigue strength by a factor 4 (low cyclic fatigue strength) and 6 (endurance limit) results from the increase of applied toughness  $\varepsilon_p \cdot R_{TZ}$  by a factor of the same rate – 5. At the same time, stress intensity factor  $K_{IC}$  is 1.8 times only. Threshold characteristics: endurance limit and threshold stress intensity factors (quantified by Eq.1.2) are given in Table 2.2.

## 2.5 Durability testing in blanking

The durability tests were carried out as service conditions (functional) ones, blanking grooves into electro-technical sheet steel with hardness 150HV, proof stress 1.6 GPa, and ultimate strength 3.2 GPa and sheet thickness 0.5 mm. The 3-position die was reinforced with three different cemented carbides to be investigated. Die was mounted on an automatic mechanical press [Appendix B, III, V, Fig.1]. The blanking performance of hardmetals was evaluated by the measure of side wear  $\Delta D$  after an intermediate service time ( $5 \cdot 10^5$  strokes) corresponded to the time between two consecutive preventive sharpening used in the exploitation of blanking dies. The side wear measurement was taken by means of the measuring machine WMM500 in constant environmental conditions as an average of 4-6 measurements.

### Results

The results of functional tests are shown in Figure 3 [Appendix B, III] as wear contours. During testing of the die, neither fracture nor brittle macrochipping of cutting edges was detected. Cutting edges became blunt as a result of uniform wear. The wear contour and the side wear data for the die tested demonstrated the obvious superiority of TiC base cermets over conventional hardmetal H15 commonly used in blanking operations. Figure 4 [Appendix B, III, V] shows the blanking performance of carbide composites opposed to their response as inserts in erosion, sliding and adhesive wear conditions.

## 2.6 Fatigue and bending strength: related fractography

The two main theories of hardmetal microstructure exist currently. Discussions about the predominance of one or another are held at present. Gurland (1963) suggested that hard carbide grains (WC) are introduced into the metallic matrix and completely isolated by binder (cobalt) from each other. This is so called *matrix structure*. These suggestions are made on the basis of WC grains excellent wettability and noticeable plasticity of WC-Co compositions with low cobalt content. The existence of carbide skeleton for the alloys with low binder content (lower than 10 %) is not denied. Also, agglomerates of joint carbide grains can be present in hardmetals with a high volume of cobalt.

The second suggestion is the existence of continuous carbide skeleton structure. Carbide frame is the continuous structure of connected (coalescent) WC grains' (content of tungsten carbide from 50wt% and higher). Slip bands found in the carbide grains during deformation proved this theory. In matrix structure reinforcement

proceeded by blocking of binder plastic deformation with carbide grains (Kreimer, 1971). The continuous carbide skeleton can be destroyed only by the fracture of a binder (possibility of binder shift is limited by tough carbide skeleton).

The dominant features of fatigue phenomena comprise not only macro-scale changes in material structure but also cover its local (micro-scale) plastic strains. In most previous studies (Sarin et al., 1974; Brooks, 1982; Loshak, 1984 etc.) the cobalt binder of WC-Co alloys has been considered as f.c.c.-metal, which in the as-sintered conditions can also deform by transforming to h.c.p. This initially gives the binder the ability to deform in full compatibility with the carbide skeleton. Ultimately the partially transformed binder is unable to fulfill the compatibility requirements and loses its ability to impede crack propagation. Since the influence of carbide grains on the bulk material fracture (monotonic and cyclic) as a whole is still undefined, the question concerning their deformation and fracture behavior arises to create an unambiguous conception about the composite constitutive behaviour. The study of the fine structure of both WC and TiC carbide phase were carried out by XRD-technique mainly used for measuring crystal lattice parameters, residual stresses and crystallite sizes. It was assumed that during monotonic and cyclic loading certain changes of these characteristics took place.

After mechanical testing selected specimens were taken and subjected to a detailed fractographic examination by scanning electron microscopy (SEM) and X-ray diffraction.

All scanning electron microscope micrographs [Appendix A, Figs.A5-A10] were made on JEOL JSM840a apparatus with following specifications:

- KV range 0.5 to 40
- magnification range 10X to 300000X
- filament type - tungsten
- resolution – 3.5 Å

The fine structure of grain is characterized by the dispersity of its crystallites, which introduced as regions of coherent dispersion of X-ray. The amount of dislocations and vacancies in lattice (microdistortions) is also a characteristic feature of crystallite. Plastic strain as the onset of fracture induces changes in grain structure by increase in dispersity of crystallites (their fragmentation) and by origin of dislocations. These changes result in alteration of the crystallite X-ray diffraction pattern: an increase in width full-width half-maximum (FWHM) of curve, characterizing the beam signal and decrease of its peak intensity.

The XRD-studies of carbide phase were carried out by the XR- diffractometer Brooks D5005. Two major alloys T70/14 and H15 were subjected to X-ray investigations. Specimens used for fatigue testing with configurations 5 x 5 x 16 mm<sup>3</sup> (T70/14) and 5 x 5 x 19 (H15) firstly were ground and then annealed in vacuum at 900°C to remove the residual stresses after grinding. Further, they were subjected for cyclic and monotonic loading at ambient temperature.

The XRD analysis layout was next:

- after grinding (standard or referent),

- after annealing,
- after fatigue testing at 80% of  $S_e$  (endurance limit) on the base of  $10^5$  cycles without fracture of a specimen,
- after fatigue testing at  $S_e$  until fracture of a specimen,
- after monotonic testing in bending until fracture (to reach the  $R_{TZ}$ ).

The XRD pattern of fractured specimen presented in Figure 2.4 were analysed a) at the maximum failure stress region (area 1) b) at the stress level of  $0,8S_e$  (area 2).

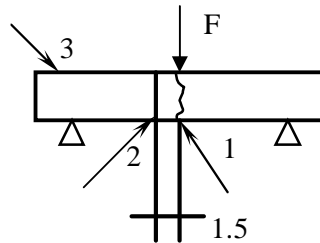


**Figure 2.4. Representation of sample areas analysed by X-Ray diffraction**

### Results

Special attention was paid to determine fracture micromechanisms associated with the different loading conditions studied.

First of all, an extended fractographic analysis indicated subsurface processing heterogeneities: pores, abnormally large carbides, binderless carbide clusters and discrete agglomerates as usual fracture initiation sites in the bending strength tests. Dimpled ductile rupture in the metallic binder interdispersed with cleavage and intergranular fracture of the carbides were the relevant fractographic features discerned in the surfaces of broken specimens, in agreement with previous investigation on this subject (Llanes *et al.*, 2000). Failure of the hard metals and cermets occurs under cyclic loading at considerably lower stress levels compared with the failure under monotonic loading. Therefore, different damage processes and damage mechanisms in the two types of loading cause this. Three fracture zones can be seen at the fracture surfaces of the specimen: a) slightly rough zone of stable crack propagation with the fracture initiation point (source of the crack); b) the zone of crack intensive propagation with coarse rough surface of fan-shape profile; c) zone of final fracture. In the first zone flaw propagates in a stable mode due to loads. The initial growth rate is low. The crack growth rate accelerates with time, but the crack remains “stable”. In this case rate-controlling factors are microstructure and applied load. The fracture surface micrographs of H10 are presented in Figure A7 [Appendix A]. The damage processes under cyclic loads are assumed to occur only in the ductile binder phase. But numerous fractured grains in the structures of both investigated hardmetals can be seen in Figures A7 and A8 [Appendix A]. This fact proves the assumptions that elastic-plastic deformation and development of slip bands in WC grains can definitely occur under cyclic loading conditions. The phase transformation and crack tip shielding by ligaments observed by Shleinkofer *et al.*, seems to be the main reason why the hardmetals show a stronger fatigue effect than the cermets in the life time depending on the stress amplitudes in the cyclic loading.

The fracture surfaces of T70/14 cermet have a mixed character. SEM micrographs show carbide grain cleavage (crack path C), the location of the crack path in the ductile binder phase (crack path B) and fracture of the phase boundary binder/ceramic (crack path B/C) Plastic deformation of thin binder layer between TiC grains is not difficult to see. But TiC grain elastic-plastic deformation traces should be examined by means of the XRD analysis. Brittle striations of T70/14 are characteristic feature of crack advancing with cycling. They are perpendicular, or almost so, to the direction to the crack propagation. Plastic striations can be observed on the little binder areas also. Plastic fracture features are visible in Figure A6 [Appendix A] as small dimples of binder phase in the lower left corner of the micrograph. As both ductile and brittle fracture features are seen, it can be assumed that under cyclic loading conditions TiC base with (Fe/Ni)-binder cermet work in the ductile-brittle transition interval.

SEM images of blanking tools are presented in Figures A9 and A10 [Appendix A]. Punches were examined after 500000 work cycles. Uniform blanking tool wear is dominant for all tested materials, but certain features of local fracture can be seen on the edges of the tested materials. In all materials, wear starts with binder extrusion-intrusion process. After adhesion between blanking tool and formed material surface tensile and shear stresses appear. As a result, influence areas of bare carbide grains can also be observed in Figures A9 and A10 [Appendix A]. In the final stage of that process, carbide grains with or without binder are extruded from the surface of the blanking tool. These areas are similar in TiC base cermet blanking tool. From Figure 9 [Appendix A] it can be noticed that edge chipping is characteristic feature of the wear process of H15 blanking dies. Cutting edges are very rough and filled with particles separated from the formed metal. On the contrary, cutting edges of T70/14 cermet are smooth and clear. There are no traces of large edge chipping processes. But small fatigue cracks are visible in the vicinity of the cutting edge. This analysis completely correlates with the numerical data obtained from both fatigue and adhesive wear testing. Wear of cutting edges of T70/14 female die is almost three times lower than that of H15 (4  $\mu\text{m}$  and 9  $\mu\text{m}$  respectively). Wear of cutting edge of T70/14 female die is approximately 2.5 times lower than that of H15 (3  $\mu\text{m}$  and 7.5  $\mu\text{m}$  respectively). Measurements were made on the depth of 0.2 mm from the upper plane of female die and lower plane of male die. On the basis of the examination it can be stated that T70/14 cermet can be accepted as a blanking tool material. It is evident fact that the adhesive wear and fatigue performance properties of this material are better than those of traditional H15 hardmetal.

XRD examination showed that after grinding remarkable changes in fine structure of both WC and TiC cermets took place [Appendix A, Fig.A11]. Fatigue tests conducted at maximum stress level 80% of endurance limit without sample fracture (on the basis of  $10^5$  numbers of cycles) did not introduce any changes in X-ray patterns of materials microstructure. The fatigue testing until fracture of specimen at the stress level of the endurance limit showed remarkable decrease of peak intensity of X-ray signal for WC phase. While changes of fine structure of TiC phase were obviously less (area 1) compared with WC one [Appendix A, Figure A12]. Monotonic testing until specimen failure resulted in sharper decrease of X-ray peak intensity (area 2) for both TiC and

WC phases. Plastic deformation of carbide phase occurs predominantly at the stress level close to material transverse rupture strength - the X-ray pattern characteristics confirm this statement [Appendix A, Figure A13].

### 3 STATISTICAL ASPECTS OF FATIGUE PERFORMANCE AND ENDURANCE LIMIT PREDICTION

#### 3.1 Statistical strength, testing procedures and Weibull modulus

To determine failure probability of heterogeneous brittle materials such as cemented carbides in varying stress fields, there are many theories, which are based on the Weibull “weakest-link” ideas. The difference between the Weibull statistics arises from the different stress states of the material during testing. The attempt to define these differences showed the evident influence of the test method and threshold stress on the Weibull modulus [Appendix B, II, Eqs.13, 16, 20]. Tests were carried out for monotonic loads with the further analysis of the test data. The cumulative probability that brittle material (with the fracture toughness below  $20 \text{ MPa}\cdot\text{m}^{1/2}$ ) fails during stressing in a uniform tension up to a stress  $\sigma$ ,  $F(\sigma)$ , is given by:

$$F(\sigma) = 1 - \exp\left[-\left(\frac{\sigma}{\sigma_0}\right)^m\right] = 1 - \exp[-S(\sigma)], \quad (3.1)$$

where  $\sigma_0$  is a normalizing parameter and  $m$  is a constant known as the Weibull modulus. It is frequently assumed that the Weibull modulus has no physical significance. Danzer *et al.* (1992) have derived an alternative formula which shows that the cumulative failure probability  $F(\sigma)$  could be given by

$$F(\sigma) = 1 - \exp[-S(\sigma)], \quad (3.2)$$

where  $S(\sigma)$  is the mean number of flaws (the presence of these flaws causes reductions in fracture toughness and strength) in a specimen during loading to  $\sigma$ . A critical or dominant flaw is one, which, satisfied some fracture criterion, e.g.  $K_I > K_{IC}$ , could be the simplest criterion of such kind. It should be noted that Weibull and Danzer’s approach could not be used to describe: a) fracture in materials, which exhibit *R*-curve behaviour or b) fracture in stabilizing stress field. It was assumed, therefore, that in both cases the initial and crack growth (the moment of fracture occurrence) flaw distributions were different. Consequently, the weakest link approach cannot be used directly to describe cracking in this case. To make the weakest link approach reliable only surface-cracking flaws were considered [Appendix B, II, Eq.9].

#### Results

In theoretical considerations, the Weibull modulus calculations in tension, three-point bending and four-point bending tests were conducted. Three plots of Weibull modulus vs. ratio maximum stress ( $\sigma_n$ ) to the lower limit of maximum stress ( $\sigma_L$ ) were obtained and presented in paper II [Appendix B, Fig.1]. The greatest increases in the Weibull modulus were expected for the three-point bending test and the smallest changes for the tension test. A confirmation of these predictions was provided by experimental results of Loshak (1984), Torres *et al.* (2002) and Preis (2000).

The differences were related to the fact that the stress is completely uniform in the tension tests. It was interesting to note that the four-point bending test is intermediate in its degree of stress uniformity. For the tension test the searched area rises from zero asymptotically towards a limit; for the four-point bending searched area has a constant component and a rising component [Appendix A, II, Eqs. 13, 16 and 20]. Thus, using a simple power-law representation for the flaw distribution, a general method for relating the Weibull modulus  $m$  to the flaw population of a brittle material was demonstrated. It showed that the Weibull modulus determined from tension, three-point bending and four-point bending tests would be equal if there is no threshold stress for fracture. The evident physical significance of the Weibull modulus was established: it is related to the rate at which cracks become critical with stress as compared to the number of cracks that are already critical. If such a stress does exist, then different test methods will give the different test values for the Weibull modulus [Appendix A, II].

### 3.2 Prediction of the lower bound of the scatter in fatigue strength: Murakami approach

In order to evaluate quantitatively the effects of defects and inclusions on the fatigue strength of various types of structural materials, Murakami (2002) suggested a new method of inclusion rating and its assessment of a correlation with the endurance limit. As explained in the description of the method, the fatigue strength can be assessed from an evaluation of the square root of the projected area of the largest defect, on a plane perpendicular to the maximum principal stress direction. This parameter, designated  $\sqrt{area}_{max}$ , contained in a definite volume, can be evaluated using the statistics of extremes of the defects distribution. By applying the method, materials can be classified according to the expected maximum size of the defect (inclusion), namely  $\sqrt{area}_{max}$  and accordingly, a prediction of the lower bound of fatigue limit can be made.

The procedure of inspection and rating of ‘surface’, ‘below the surface’ and ‘interior’ defects is complicated one. A section perpendicular to the maximum normal stress is cut from the specimen. After sample preparation, the SEM pictures of the inspection area ( $A_0$ ) are chosen [Appendix A, Fig.A2]. Generally it is a microscopic picture of an area approximately equivalent to  $A_0$ . In this area, a defect of maximum size is selected. Then the square root of the projected area is calculated. This operation is repeated  $n$  times. The values of  $\sqrt{area}_{max}$  are classified, starting from the smallest, and indexed. The cumulative probability function  $F_j$  and the reduced variates  $y_j$  are then calculated from the equations:

$$F_j = j \times 100 / (n + 1)\% , \quad (3.3)$$

$$y_j = -\ln \left\{ -\ln \left[ j / (n + 1) \right] \right\} , \quad (3.4)$$

The data are then used in calculating the lower band of the scatter of fatigue limit. All the formality of technique applied is presented in Appendix A, Table A1. The cobalt

binder Vicker's hardness was measured for the final calculation of lower bound of endurance limit. In this prediction procedure only one WC-base hardmetal was examined. Its defect areas were measured by means of transporting the SEM images of samples into AutoCAD interface, and resulted in the calculation and rating of the size of the defect areas [Appendix A, Fig.A3].

### **Results**

The possibility of using  $\sqrt{area_{max}}$  as the geometrical parameter was suggested in the prediction of the fatigue strength of H15 hardmetal presented. As was described above, if one accepts that the fatigue limit of a material containing small defects or cracks is the threshold condition for non-propagating cracks, then it is rational to consider the most appropriate material parameter for describing the threshold behaviour. From the trends of the correlation of  $HV$  with the stress intensity factor (for most metallic bulk materials) it was assumed that this parameter of Co-binder of WC-Co composite might suit for fatigue strength assessment. In addition, the adhesion wear of carbide composite is controlled, first of all, by properties of its binder (intrusion-extrusion mechanism of adhesion). The results of equating the lower band of scatter of fatigue strength ( $S_e \approx 590$  MPa) on the basis of Vickers hardness and geometric parameter  $\sqrt{area_{max}}$  showed its excellent convergence with experimental data received from both the testing procedure of standard fatigue tests ( $S_{e,min} \approx 720$  MPa) and accelerated fatigue ones ( $S_e \approx 500$  MPa).

## CONCLUSIONS

1. In the study carried out it was shown that the fatigue performance of cemented carbides has to be taken into account if an evaluation of reliability is required.
2. The dominant feature of fatigue phenomenon of heterogeneous materials is that the onset of failure starts and takes place mainly in the binder phase.
3. During cyclic loading the cobalt binder phase of WC-base alloy deforms by transformation from f.c.c to h.c.p. crystal structure with ligament zone formation. As a result, this transformation decreases the ability of binder to impede crack propagation. On the other hand, the most part of carbide phase is deformed in the immediate region of fracture stress with high level of plastic strain energy accumulated. Consequently, a higher magnitude of transverse rupture strength ( $R_{TZ}$ ) is typical of WC-Co composite.
4. In its turn, the lower fatigue sensitivity of TiC-base cermet can be explained by the absence of such a Fe/Ni-binder phase transformation as of cobalt binder. At the same time, more brittle TiC-phase gives the lower value of bulk material  $R_{TZ}$ .
5. Better blanking performance of TiC-base cermet with steel binder can be attributed to its lower fatigue sensitivity. It was also shown that the fatigue sensitivity of cermets is controlled by the plasticity of bulk materials.
6. A recent study has shown that the adhesive wear fracture of cemented carbides starts like fatigue does – predominantly in the binder phase (extrusion-intrusion mechanism) and in contrast to abrasive erosion and sliding wear. In this case, the properties of binder (strength and adhesive interaction) are of more interest than those of the carbide phase. Reasonable correlation between the blanking performance and adhesive wear resistance, and similarity in the surface failure morphology was found. Local microfailure zones result in the microchipping of cutting edges during blanking. Microchipping in its turn causes an increase in shear stresses, resulting in the acceleration of tool wear.
7. The X-ray examinations stated that the plastic strain – onset of failure of WC- and TiC-base cemented carbides during cyclic loading starts and takes place mainly in the binder phase. The carbide phases do not undergo any plastic strain during cyclic loading at the stress levels below the fracture stress. The considerable plastic strain of carbide phase under cyclic load conditions occurs predominantly at the stress level close to material fracture stress. The critical

plastic strain of WC-phase of WC-15wt%Co composition exceeds that of TiC-one. The tungsten carbide phase is more plastic compared to the TiC one.

8. The new technique developed by Murakami (2002) for the prediction of the lower bound of endurance limit of WC-Co hardmetal was applied. It was accepted that the endurance limit of a material containing small defects, inclusions or cracks is the threshold condition for non-propagating cracks. The Vicker's hardness of cobalt binder (as main responsible for the fracture characteristic) and geometrical parameter of maximum area of structural defect were assumed to be the basis of such calculations. The results of this procedure showed excellent convergence with experimental data received from both testing procedure of standard fatigue tests and accelerated fatigue ones.

## REFERENCES

- Almond, E., and Roebuck, B. (1981). Fatigue crack growth in WC-Co. *Metals Technology*. 2: 83-85.
- Baily, R. (1951). Creep relationships and their application to pipes, tubes and cylindrical parts under internal pressure. *Journal of European Ceramic Society*. London. 36-47
- Brookes, K., (1982) *World dictionary and handbook of hardmetals and hard materials*. 5<sup>th</sup> ed. London: International Carbide Data
- Brooks, K. (1996). *World dictionary and handbook of hardmetals and hard materials*. 6<sup>th</sup> ed. London: International Carbide Data.
- Danzer, R (1992). A general strength distribution function for brittle materials. *Journal of European Ceramic Society*. 10: 461-472
- DIN 51110 *Maximum Likelihood Estimation of Weibull Modulus static, monotonic and cyclic loading. Brittle materials*.
- Dowling, N. (1998). *Mechanical behaviour of materials*. New Jersey. 1999
- Exner, H. and Walter, A. and Pabst, R. (1974). Zur ermittlung und darstellung der fehlerverteilungen von spröden werkstoffen. *Materials Science and Engineering*. 8: 925-934.
- Fox-Rabinovich, G. and Kovalev, A. (1994). Characteristic features of blanking die wear with consideration for the change in composition, structure and properties of contact surfaces. *Wear*. 189: 25-31.
- Fry, P. and Garret, G. (1983). The inter-relation of microstructure, toughness and fatigue crack growth in WC-co hardmetals. *Proceedings of the International Conference on Speciality Steels and Hard Materials*. London. Pergamon. 375-381.
- Gurland J. (1963) The fracture strength of sintered WC-Co alloys in relation to composition and particle spacing.- *Transactions of Metallurgical Society*. 227.10. 1063-1071.
- Hirose, Y., Boo, M., Matsuoka, H. and Park, Y. (1997). Influence of stress ratio and WC grain size on fatigue crack growth characteristics of WC-Co cemented carbides. *Journal of Society of Materials Science in Japan*. 46: 1402-1409
- Ishihara, S., Goshima, T., Yoshimoto, T. and Sabu, T. (1999) On fatigue lifetimes and crack growth behaviour of cemented carbides. *Fatigue'99. Proceedings of the 7<sup>th</sup> International Fatigue Congress*. Beijing. 1811-1816.
- ISO 3327 (ASTM B406) *Transverse Rupture Strength Determination: Cemented Carbides*.
- Kenny, P. (1971) The application of fracture mechanics to cemented carbides. *Powder Metallurgy*. 14: 22-38.

- Knee, N. and Plumbridge, W. (1984). The influence of microstructure and stress ratio on fatigue crack growth in WC-Co hardmetals. *Proceedings of the 6<sup>th</sup> International Conference on Fracture*. New Delhi. 2685- 2692.
- Kreimer, H. (1971). Strength of hardmetals. Moscow: Metallurgiya (in Russian).
- Kursawe, S., Pott, Ph., Sockel, H. G., Heinrich, W., Wolf, M. (2001). On the influence of binder content and binder composition on the mechanical properties of hardmetals. *International Journal of Refractory Metals & Hard Metals*. 19: 335-340.
- Lawn, B. (1993). *Fracture of brittle solids*. 2<sup>nd</sup> edition. Cambridge. Cambridge University Press.
- Llanes, L. Torres, Y., Anglada. (2002). On the fatigue crack growth behavior of WC-Co cemented carbides: kinetics description, microstructural effects and fatigue sensitivity. *Acta Materialia*. 50: 2381-2393.
- Llanes. L., Torres, Y., Casas, B., Casellas, D., Marimon, F., Roure, F., and Anglada M. (2001). Fracture behaviour of cemented carbides: a fracture mechanics analysis. *Proceedings of the 13<sup>th</sup> European Conference of Fracture, Fracture Mechanics: Applications and Chalanges*. San Sebastian: Elsevier. ECF 13 on CD-ROM.
- Loshak, M. (1984). Strength and durability of hardmetals. Kiev: Naukova Dumka (in Russian).
- Murakami, Y. (2002) *Fatigue of metals*. London. Elsevier.
- Preis, I. (2000). *Assessment of fatigue characteristics of cemented carbides*. Thesis for the degree of Master of Science in Engineering. Tallinn.
- Reshetnyak, H. and Kübarsepp, J. (1997). Structure sensitivity of wear resistance of hardmetals. *International Journal of Refractory Metals & Hard Materials*. 15: 89-98.
- Reshetnyak, H. and Kübarsepp, J. (1998). Resistance of hardmetals to fracture. *Powder Metallurgy*. 41: 211-216.
- Sarin, V. (1974). *Metall Science*. 9: 472-476.
- Shleinkofer, U., Sockel H., Görting, K. and Heinrich, W. (1996). Fatigue of hardmetals and cermets. *Materials Science and Engineering*. A, 209: 313-317.
- Shleinkofer, U., Sockel H., Görting, K. and Heinrich, W. (1997). Fatigue of hardmetals and cermets – new results anf better understanding. *International Journal of Refractory Metals and Hard Materials*. 15: 103-112.
- Shleinkofer, U., Sockel H., Görting, K. and Heinrich, W. (1996). Microstructural processes during subcritical crack growth in hard metals and cermets under cyclic loads. *Materials Science and Engineering*. A, 209: 103-110.
- Shleinkofer, U., Sockel H., Schlund, P., Görting, K. and Heinrich, W. (1995). Behaviour of hardmetals and cermets under cyclic mechanical loads. *Materials Science and Engineering*. A, 194:1-8.

- Sigl, L. and Exner, H. (1987). Experimental study of the mechanics of fracture in WC-Co alloys. *Metall Transactions*. 18. 1299-1308.
- Sigl, L. and Fishmeister, H. (1988) On the fracture toughness of cemented carbides. *Acta Metallurgica*. 36: 887-897.
- Suresh, S. (1991). *Fatigue of materials*. Cambridge: Cambridge University Press
- Torres, Y., Anglada, M. and Llanes, L. (2001). Fatigue mechanics of WC-Co cemented carbides. *International Journal of Refractory Metals & Hard Materials*. 19: 341-348.
- Torres, Y., Casellas, D., Anglada M. and Llanes L. (2000). Fracture toughness evaluation of hardmetals: influence of testing procedure. *International Journal of Refractory Metals and Hard Materials*. 19: 27-34.
- Weibull, W. (1941). A statistical distribution function of wide application. *Journal of Applied Mechanics*. 18: 293-297
- Zhurkov, S. (1965). Kinetik concept og the sthrength of solids. *International Journal of Fracture Mechanics*.4:66-71

## SYMBOLS AND ABBREVIATIONS

### Symbols

- $d_{WC}$  – mean tungsten carbide grain size  
 $E$  – Young's modulus  
 $F$  – probability of failure  
 $\sqrt{area}_{max}$  - maximum size of the defect area(Murakami's parameter)  
 $\nu$  – Poisson's ratio  
 $\sigma$  – applied stress (nominal)  
 $\sigma_0$  – normalized parameter of inert strength (Weibull statistics)  
 $\sigma_{max}$  – maximum applied stress  
 $\sigma_{min}$  – minimum applied stress  
 $\sigma_m$  - mean applied stress  
 $\Delta\sigma$  – applied stress range  
 $\Delta\sigma_{th}$  – applied threshold stress (range)  
 $R_{TZ}$  – transverse rupture strength  
 $\sigma_a$  – stress amplitude  
 $R_{CM}$  – compressive strength  
 $R_{C0.1}$  – proof stress in compression  
 $\sigma_a$  – stress amplitude  
 $\sigma_m$  – mean stress  
 $\sigma_f$  – fatigue limit (strength)  
 $\tau$  - shear stress  
 $K$  – stress-intensity factor  
 $K_c$  – fracture toughness  
 $K_{Ic}$  – plane-strain fracture toughness  
 $K_{th}$  – threshold stress intensity factor  
 $K_f$  – fatigue limit stress intensity factor  
 $\Delta K_{th}$  – range of threshold stress intensity factor  
 $m$  – Weibull modulus  
 $m_0$  – Weibull modulus of monotonic testing  
 $m_c$  – Weibull modulus of cyclic testing  
 $N$  – number of elapsed stress cycles  
 $N_f$  – fatigue life (cycles)  
 $R$  – stress ratio

- $\lambda_{\text{co}}$  – binder thickness, of cobalt in WC-Co cemented carbides  
 $C_{\text{WC}}$  – carbide contiguity, of tungsten carbide skeleton in WC-Co cemented carbides  
 $V_{\text{co}}$  – volume of cobalt binder  
 $\varepsilon_{\text{p}}$  – ultimate plastic strain  
 $\rho$  – density  
 $S_{\text{e}}$  – endurance (fatigue limit)  
 $S_{\text{max}}$  – maximum nominal stress  
 $S_{\text{b}}$  – inert bending strength,  
 $S(\sigma)$  – mean number of surface flaws

### **Abbreviations**

- ASTM – American Standards of Testing Methods  
FCG – Fatigue Crack Growth  
HRA – Rockwell hardness number  
HV – Vickers hardness number  
SEM – Scanning Electron Microscope  
ISO – International Standardization Organization  
DIN – German industry standard (Deutsche Industrie Norm)

## **APPENDIX A**

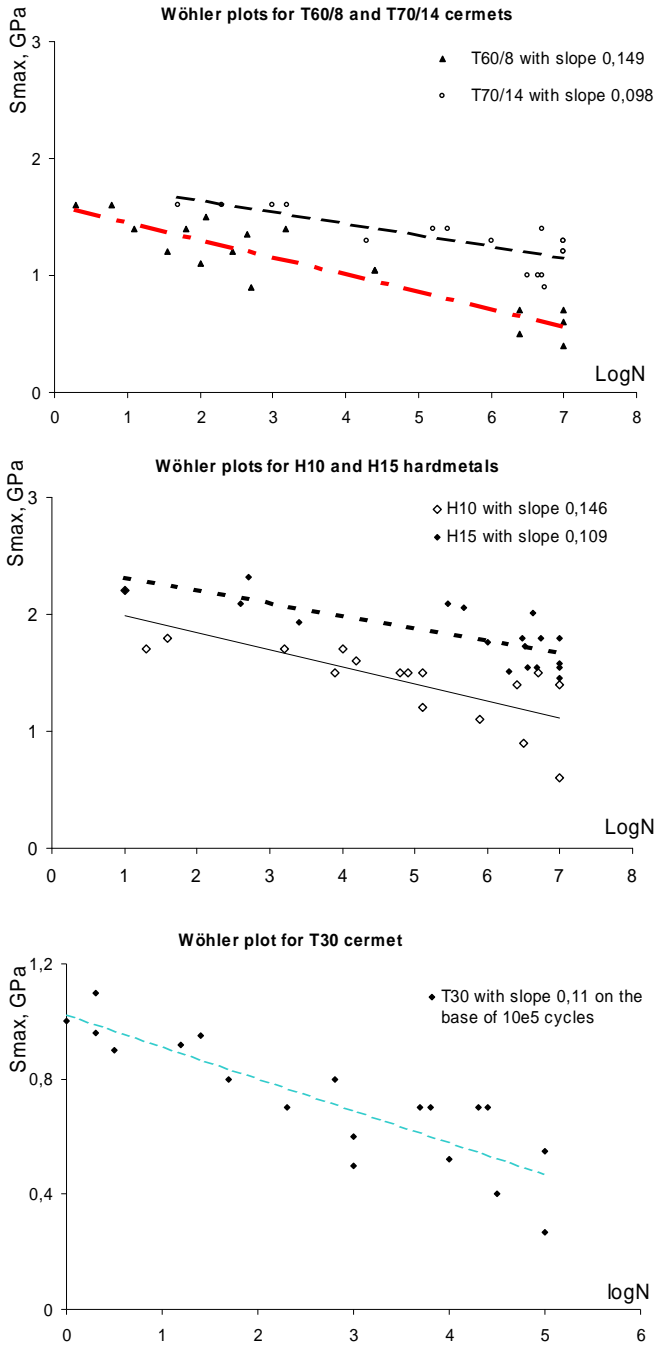


**Figure A1. Wöhler plots for TiC-base and WC-base hardmetals.**

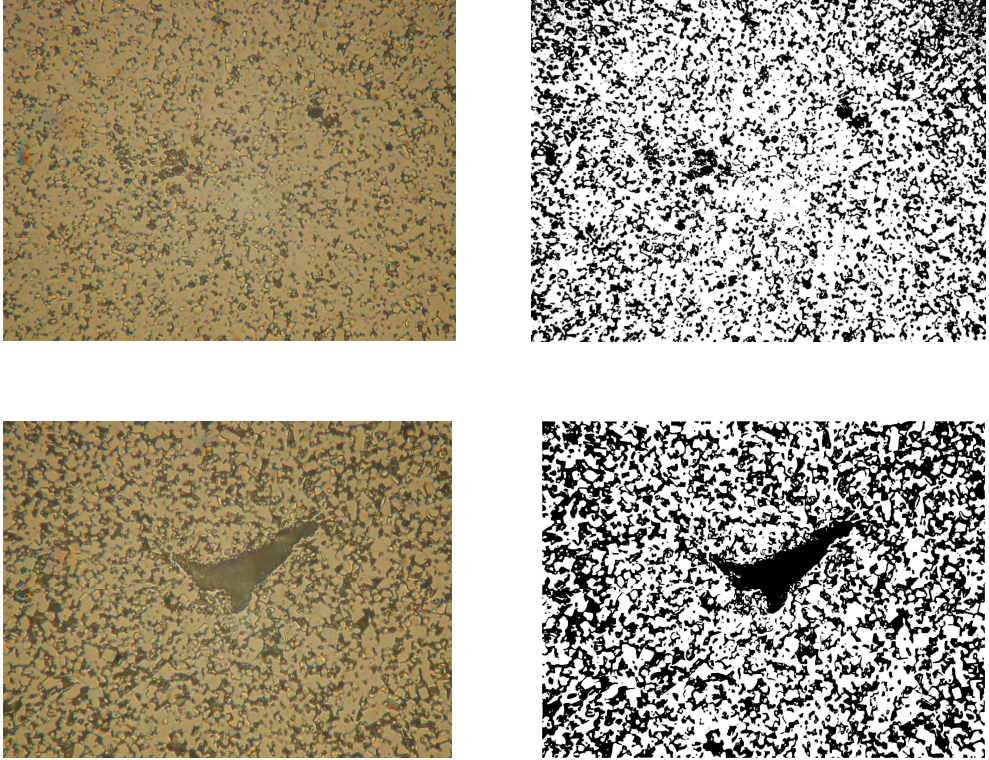


**Figure A2. Samples of SEM images of the inspection area for hardmetal H15**

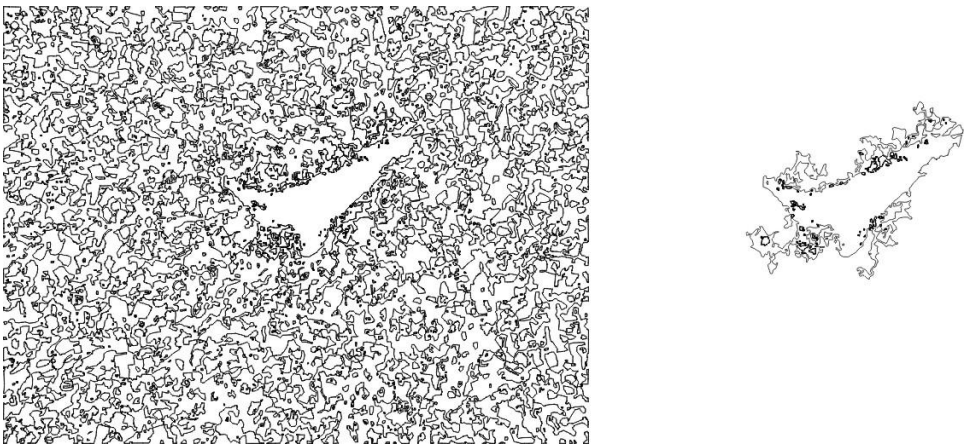


**Figure A3. Images of area of defects imported to AutoCAD for the defect area calculations**

**Table A1. Defects inspection items**

<b>Inspection items</b>
<b>Material: H15, WC- 15wt %Co</b> Control section: Transverse to normal stress Standard inspection area: 0.134 mm <sup>2</sup> Number of inspections: n=99
<b>Maximum defect distribution</b>
$\sqrt{area}_{max} = 33.006y + 55,665$ Test area: A (mm <sup>2</sup> ) Return period: T = A/A <sub>0</sub> Cum. Distr. Func. $F_j = j \times 100 / (n+1)\%$ Reduced variate $y_j = -\ln\{-\ln[j/(n+1)]\}$

**Table A1. Defects inspection items (continue)**

<b>Prediction of <math>\sqrt{area}_{max}</math></b>		
A (mm <sup>2</sup> )	T	$\sqrt{area}_{max}$ (μm)
1	7.44	119.552
10	74.41	197.682
100	744.01	273.883
<b>Prediction of lower bound of the scatter in fatigue strength Co – binder <math>H_V = 174</math></b>		
$S_e = 1.43(H_V + 120)/(\sqrt{area})^{1/6}$ for surface defects MPa	$S_e = 1.41(H_V + 120)/(\sqrt{area})^{1/6}$ for defects just below the surface, MPa	$S_e = 1.56(H_V + 120)/(\sqrt{area})^{1/6}$ for interior defects, MPa
$S_{e1} = 598$	$S_{e1} = 590$	$S_{e1} = 652$
$S_{e10} = 550$	$S_{e10} = 542$	$S_{e10} = 600$
$S_{e100} = 521$	$S_{e100} = 513$	$S_{e100} = 568$

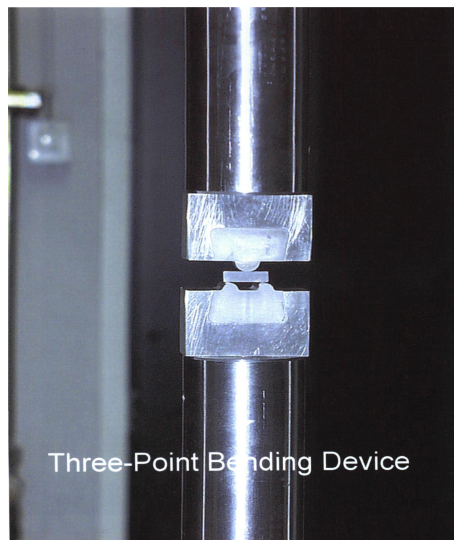
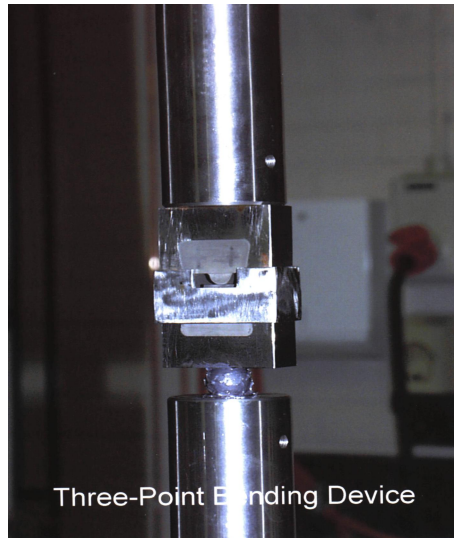


**Figure A4. Standard three-point bending device used in cyclic and monotonic testing**

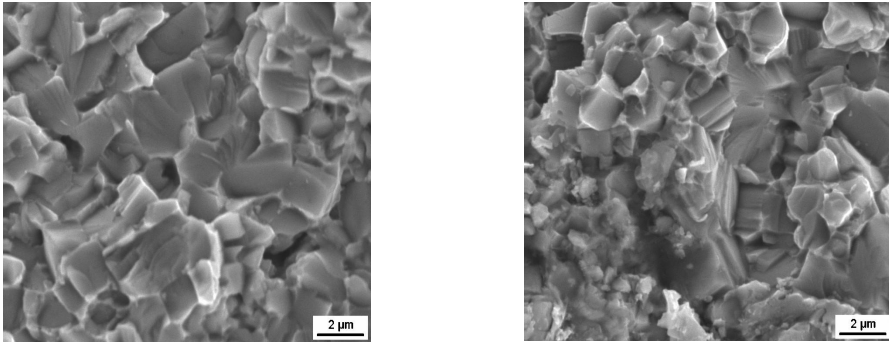


**Figure A5. SEM micrographs of fracture surfaces of cermet T70/14 that failed under cyclic loads (a) with traces of binder plastic deformation (b)**

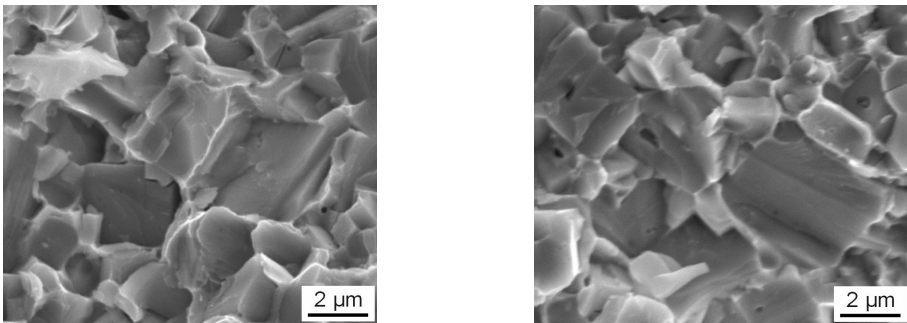


**Figure A6. SEM micrographs of fracture surfaces of cermet T70/14 with a visible plastic deformation of thin binder layers (a) and pores and flaws visible (b)**

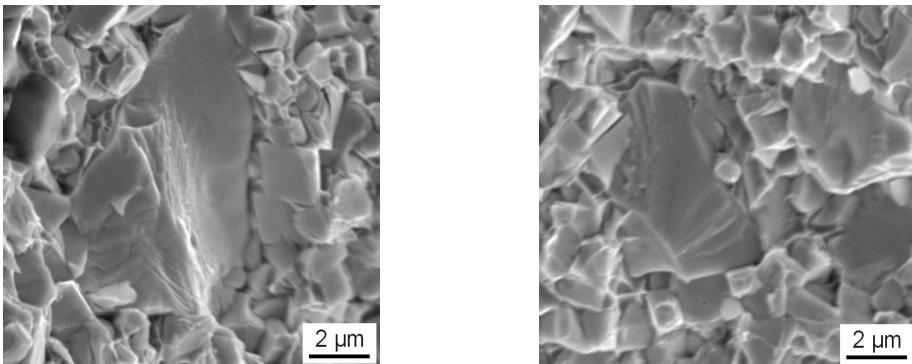


**Figure A7. SEM micrographs of fracture surface of H10 with striations observed in the WC phase (a) and signs of WC phase cleavage (b)**

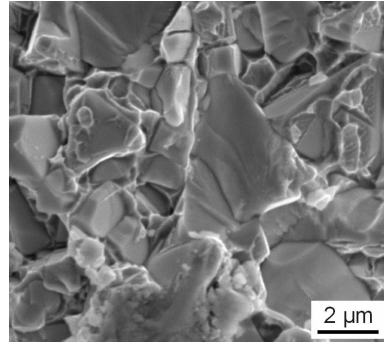
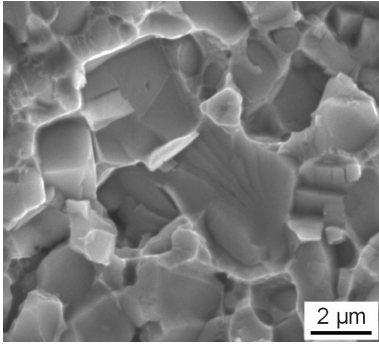


**Figure A8. SEM micrographs of fracture surfaces of H15 with traces of WC phase brittle fracture (a) and WC grain slip bands traces (b)**

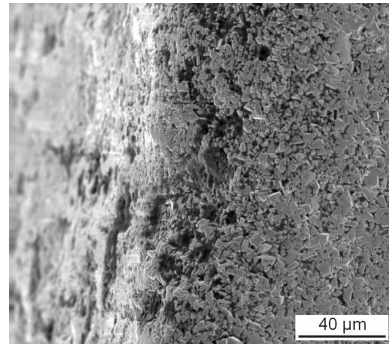
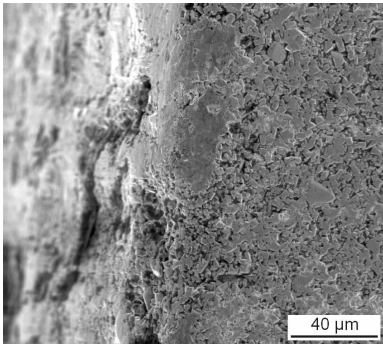


**Figure A9. SEM micrographs of H15 female (a) and male (b) die wear of cutting edges**

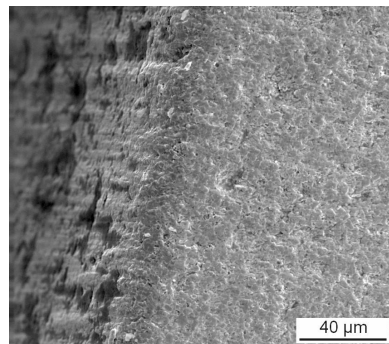
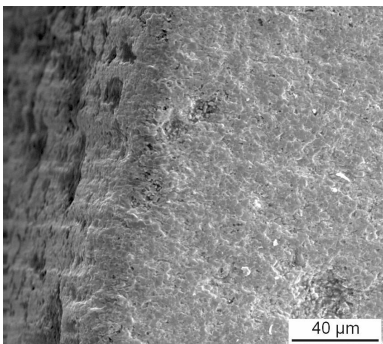


**Figure A10. SEM micrographs of T70/14 female (a) and male (b) die wear of cutting edges**

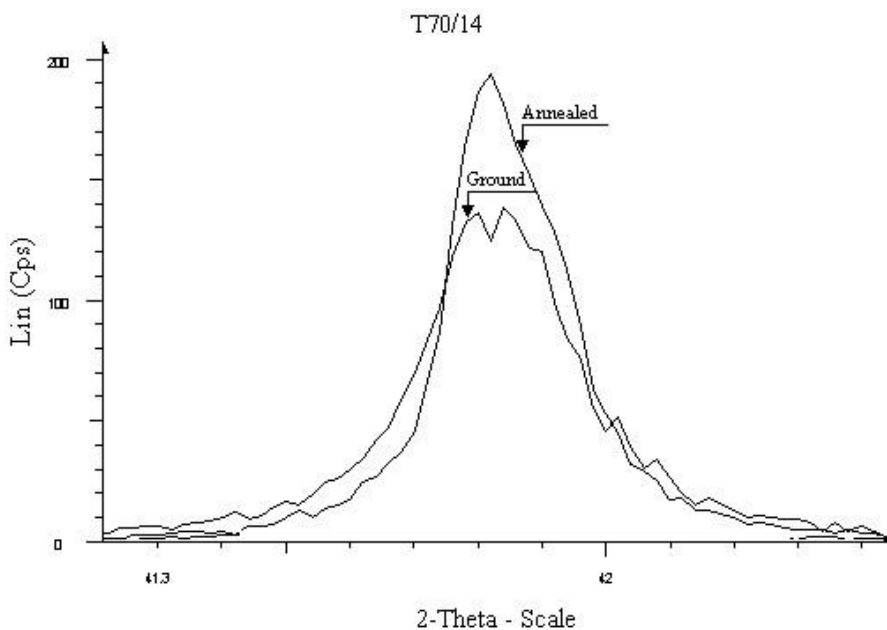
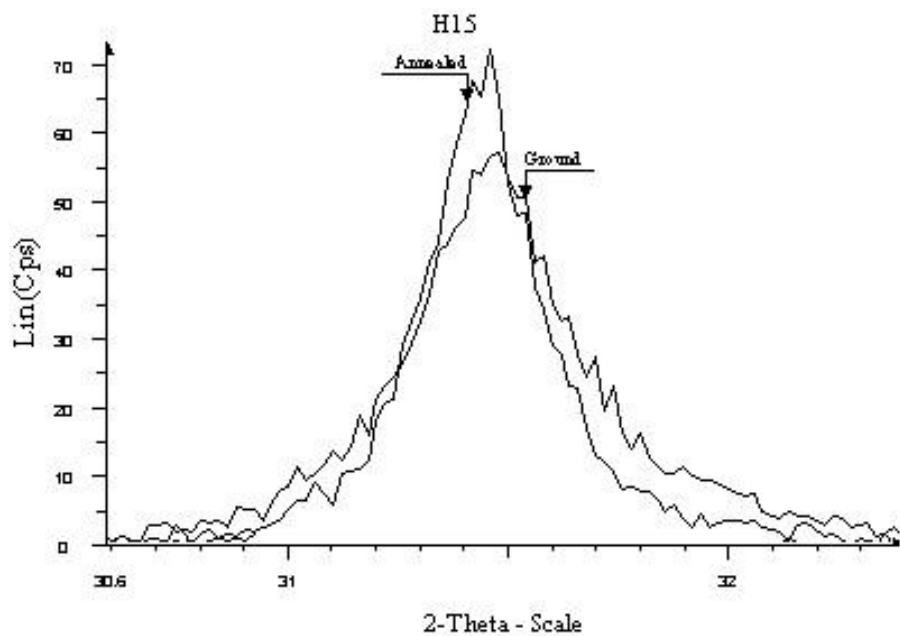
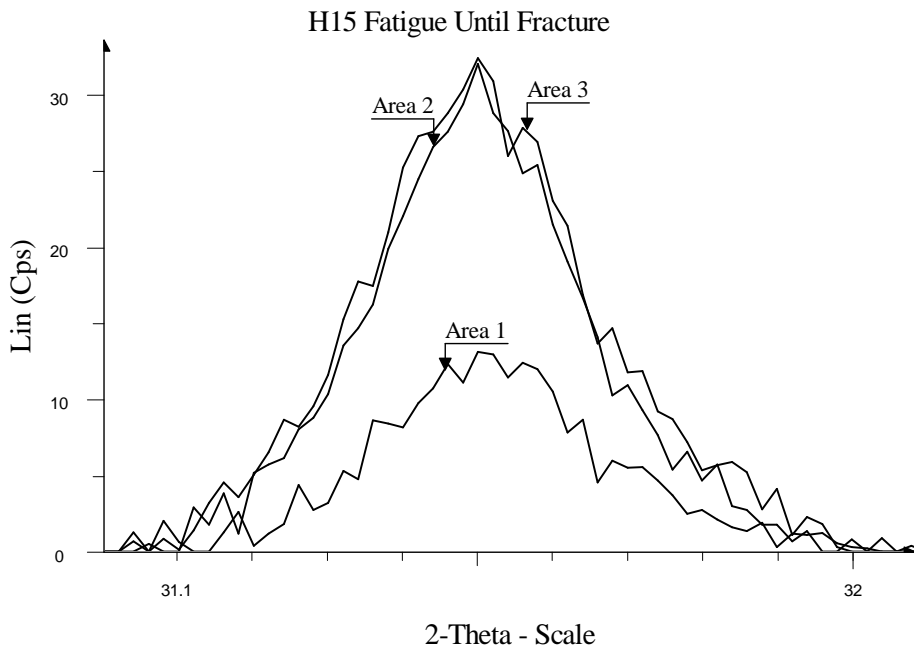
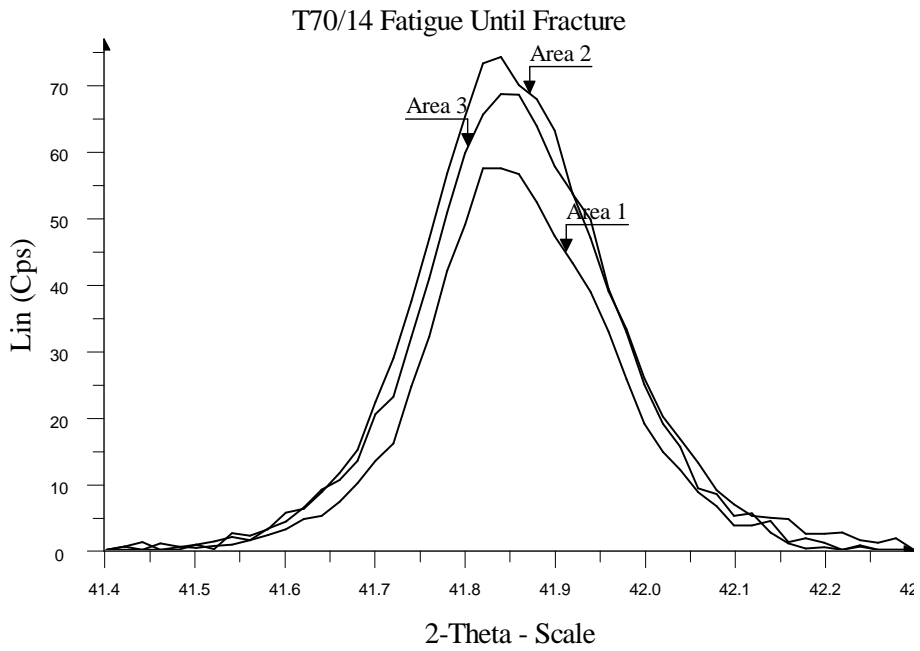
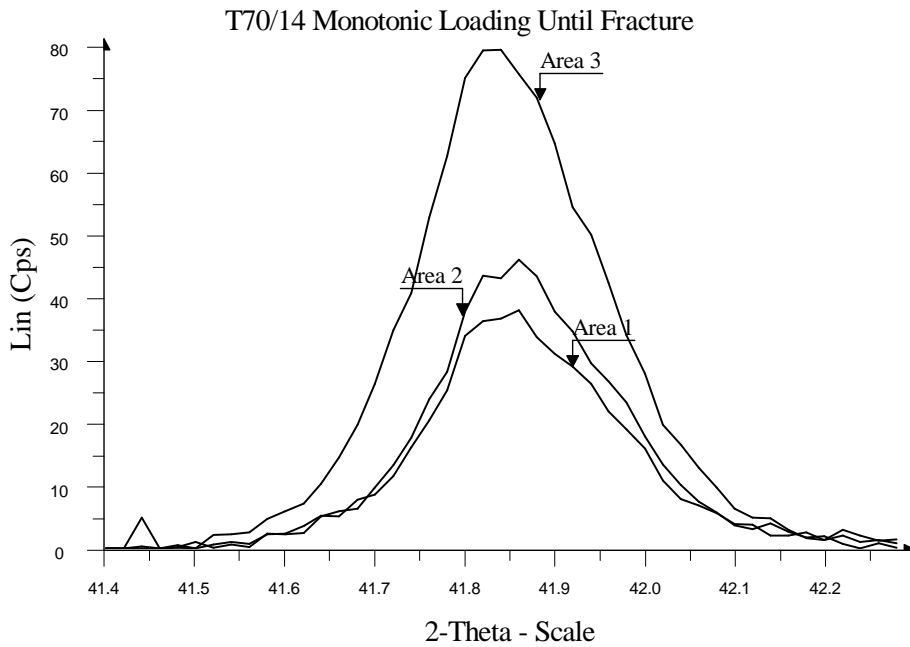
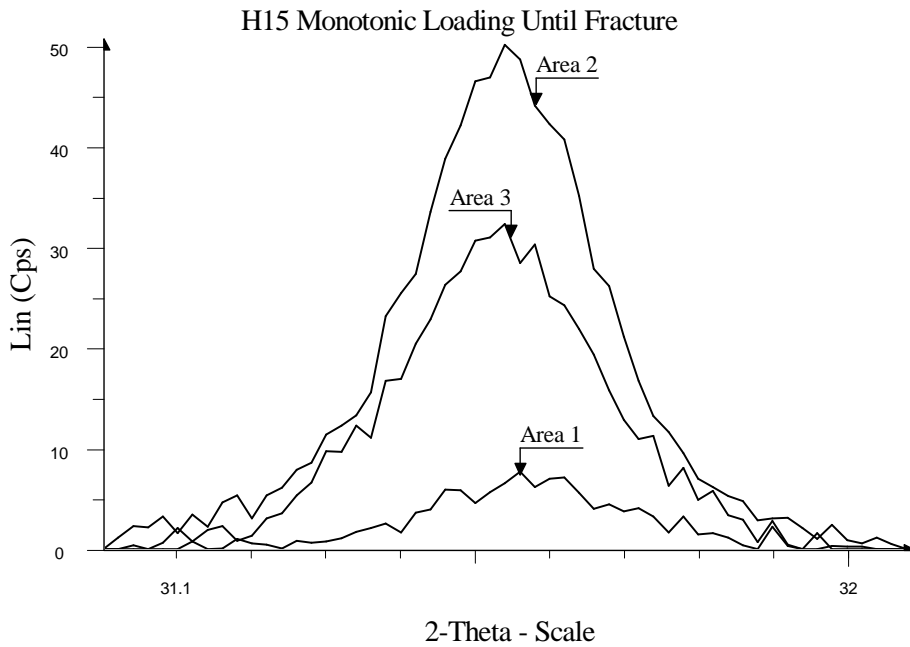


Figure A11. X-Ray pattern of ground and annealed carbide phase of cemented carbides



**Figure A12.X-Ray patterns of carbide phases fractured under cyclic loading conditions**



**Figure A13. X-Ray pattern of carbide phase fractured under monotonic loading conditions**

## **APPENDIX B**

## CURRICULUM VITAE (CV)

*Name* Irina  
*Surname* Preis  
*Contact* Virbi 20-50 13629, Tallinn, Estonia;  
 Telephone: +372 6325 650: E-mail: ipreis@edu.ttu.ee  
*Workplace* Tallinn University of Technology, Department of Materials  
 Engineering, Ehitajate tee 5, 19086 Tallinn  
*Appointment* Teaching Assistant  
*Date and place of birth* 08.08.1966, Kaliningrad, Russia  
*Citizenship* Estonian  
*Family status* Married

### Education history

<i>Educational institution</i>	<i>Year of graduation</i>	<i>Education</i>
School N7, Kaliningrad	1983	Secondary-level Educations
Tallinn Polytechnic Institute, Faculty of Mechanical Engineering	1989	Engineer
Tallinn Technical University, Faculty of Mechanical Engineering	2000	M.Sc. (Eng)
Tallinn Technical University, Estonian Centre for Engineering Pedagogy	2002	Engineering educator in information- communication technology (ICT).

### Work experience

<i>Employment time</i>	<i>Organisation</i>	<i>Appointment</i>
1998 – present time	Tallinn University of Technology	Teaching Assistant
1995-1998	Tallinn Technical University	Technician
1988-1995	Specialized Design Bureau “ Effect”	Engineer- Designer

*Scientific degree* Master of Science in Engineering  
*Certificate of education* Tallinn Technical University, 2000  
*Scientific Work* Fatigue and durability of powder metallurgy  
 materials - cemented carbides

*List of most important publications*

1. I.Preis, J.Kübarsepp, V. Strižak, Preliminary assessment of durability of hardmetals and cermets. Proc. of the 3 rd Int. Conf. on Industrial Engineering - New Challenges to SME, April 27-29, 2000, Tallinn, Estonia, pp. 175-178.
2. H. Klaasen, J. Kübarsepp, I. Preis, Toughness of carbide composites and their durability in application. Proc. of European Conf. on Hard Materials and Diamond Toolin, EURO PM 2002, October 7-9, 2002, Lausanne, Switzerland, European Powder Metallurgy Association, 210-245.
3. H. Klaasen, J.Kübarsepp, I.Preis, Toughness and durability of cemented carbides. Proc. of the Int. Conf. on Deformation and Fracture of Structural PM Materials, September 15-18, 2002, Slovak Republic, IMR SAS - European Powder Metallurgy Association, Kosice, Vol. 1, pp.77-83.
4. H.Klaasen, J.Kübarsepp, I.Preis, Durability in application of TiC-base cermets. Proc. of World Congress and Exhibition on Powder Metallurgy PM 2004, October 17-22, Vienna, Austria, European Powder Metallurgy Association
5. H. Klaasen, J.Kübarsepp, I.Preis , Toughness characteristics of carbide composites. Proc. of 3 rd Int. Conf. on Industrial Engineering - New Challenges to SME, April 25-27, 2002, Tallinn, Estonia, pp. 154-156.
6. Preis, Statistical strength of brittle materials:test methods and Weibull modulus. Proc. of 3 rd Int. Conf.- New Challenges to SME, April 25-27, 2002, Tallinn, Estonia, pp.205-208.
7. I.Preis, F.Sergejev, Microstructural aspects of fatigue mechanics of hardmetals and cermets. Proc. of the 2 nd Symposium on Experimental Solid Mechanics, Milano Marittima, Italy, 2003, pp. 172-174.
8. H.Klaasen, J.Kübarsepp and I.Preis, Durability of advanced TiC-base cermets. Proc. of the Estonian Academy of Sciences. Engineering, 9 (4), 2003, 272-280.

9. I.Preis, F.Sergejev, Failure of brittle materials: test methods and Weibull modulus. Proc. of the 3 rd Youth Symposium on Experimental Solid Mechanics, Poretta Terme, Italy, 2004, pp. 115-117.
  
10. H. Klaasen, J.Kübarsepp, I.Preis, Wear behaviour, durability and cyclic strength of TiC base cermets. Materials Science and Technology, v 20 (August) 2004

## ELULOOKIRJELDUS (CV)

*Eesnimi* Irina  
*Perekonnanimi* Preis  
*Kontaktandmed* Virbi 20-50, Tallinn, 13629; tel.+372 6325 650; E-mail:  
ipreis@edu.ttu.ee  
*Töökoht* TTÜ Materjalitehnika, Ehitajate tee 5, 19086 Tallinn  
*Ametikoht* Assistent  
*Sünniaeg ja koht* 08.08.1966, Kaliningrad, Venemaa  
*Kodakondsus* Eesti  
*Perekonnaseis* Abielus

### Hariduskäik

<i>Õppeasutus</i>	<i>Lõpetamise aeg</i>	<i>Haridus</i>
Kaliningradi keskkool N7	1983	keskharidus
Tallinna Polütehniline Instituut, mehaanikateaduskond	1989	mehaanikainsener
Tallinna Tehnikaülikool, mehaanikateaduskond	2000	Tehnikateaduste magister
Tallinna Tehnikaülikool, Eesti Inseneripedagoogika keskus	2002	info- ja kommunikatsiooni-tehnoloogia valdkonna õpetaja

### Teenistuskäik

<i>Töötamise aeg</i>	<i>Organisatsiooni nimetus</i>	<i>Ametikoht</i>
1998-käesoleva ajani	Tallinna Tehnikaülikool, Materjalitehnika instituut	assistent
1995-1998	Tallinna Tehnikaülikool, Keemiatehnika instituut	laborant
1988-1995	Spets. Kontrüeerimis Büroo "Effect"	insener

*Teaduskraad* Tehnikateaduste magister  
*Teaduskraadi välja andnud asutus, aasta* Tallinna Tehnikaülikool, 2000  
*Teadustöö suund* Karbiidkermiste väsimustugevus.

## Artiklid

1. I.Preis, J.Kübarsepp, V. Strižak, Preliminary assessment of durability of hardmetals and cermets. Proc. of the 3 rd Int. Conf. on Industrial Engineering - New Challenges to SME, April 27-29, 2000, Tallinn, Estonia, pp. 175-178.
2. H. Klaasen, J. Kübarsepp, I. Preis, Toughness of carbide composites and their durability in application. Proc. of European Conf. on Hard Materials and Diamond Toolin, EURO PM 2002, October 7-9, 2002, Lausanne, Switzerland, European Powder Metallurgy Association, 210-245.
3. H. Klaasen, J.Kübarsepp, I.Preis, Toughness and durability of cemented carbides. Proc. of the Int. Conf. on Deformation and Fracture of Structural PM Materials, September 15-18, 2002, Slovak Republic, IMR SAS - European Powder Metallurgy Association, Kosice, Vol. 1, pp.77-83.
4. H.Klaasen, J.Kübarsepp, I.Preis, Durability in application of TiC-base cermets. Proc. of World Congress and Exhibition on Powder Metallurgy PM 2004, October 17-22, Vienna, Austria, European Powder Metallurgy Association
5. H. Klaasen, J.Kübarsepp, I.Preis , Toughness characteristics of carbide composites. Proc. of 3 rd Int. Conf. on Industrial Engineering - New Challenges to SME, April 25-27, 2002, Tallinn, Estonia, pp. 154-156.
6. Preis, Statistical strength of brittle materials:test methods and Weibull modulus. Proc. of 3 rd Int. Conf.- New Challenges to SME, April 25-27, 2002, Tallinn, Estonia, pp.205-208.
7. I.Preis, F.Sergejev, Microstructural aspects of fatigue mechanics of hardmetals and cermets. Proc. of the 2 nd Symposium on Experimental Solid Mechanics, Milano Marittima, Italy, 2003, pp. 172-174.
8. H.Klaasen, J.Kübarsepp and I.Preis, Durability of advanced TiC-base cermets. Proc. of the Estonian Academy of Sciences. Engineering, 9 (4), 2003, 272-280.
9. I.Preis, F.Sergejev, Failure of brittle materials: test methods and Weibull modulus. Proc. of the 3 rd Youth Symposium on Experimental Solid Mechanics, Poretta Terme, Italy, 2004, pp. 115-117.
10. H. Klaasen, J.Kübarsepp, I.Preis, Wear behaviour, durability and cyclic strength of TiC base cermets. Materials Science and Technology, v 20 (August) 2004

## **ARTICLE I**

## **ARTICLE II**

## **ARTICLE III**

## **ARTICLE IV**

## **ARTICLE V**